PERGAMON

Journal of Structural Geology 24 (2002) 1065–1085

JOURNAL OF STRUCTURAL GEOLOGY

www.elsevier.com/locate/jstrugeo

Competency contrast, kinematics, and the development of foliations and lineations in the crust

Laurel B. Goodwin[a,*], Basil Tikoff[b]

[a]Department of Earth and Environmental Science, New Mexico Tech, Socorro, NM 87801, USA
[b]Department of Geology and Geophysics, University of Wisconsin, Madison, WI 53706, USA

Received 16 January 2001; revised 20 July 2001; accepted 30 July 2001

Abstract

Similar foliation patterns are observed in faults in poorly lithified sediments, fault gouge and cataclasite, and greenschist to granulite facies shear zones. We suggest that this similarity in form reflects similar controls on development. We propose that these patterns are a fundamental consequence of deformation of heterogeneous media, in which material heterogeneity is manifest as competency contrast. Strain incompatibilities along competence domain boundaries can produce mechanical instabilities, resulting in the nucleation of shear bands and/or *C*-surfaces. Mechanical segregation of incompetent material into these foliations produces compositional bands.

Competency contrast promotes strain partitioning between compositional bands, accommodated in part by domain-boundary sliding. In three-dimensional general shear, incompetent domains and domain boundaries will preferentially accommodate the non-coaxial component of flow, and strain rates will be higher than in competent domains. Consequently, lineations in incompetent domains are different from, and may be orthogonal to, those in competent domains. Lineations that record tectonic transport will form preferentially in incompetent domains; lineations in more competent domains may (if not steady-state) approximate the long axis of the finite strain ellipsoid of the competent domains. The number and orientations of foliations and lineations, and microstructures that record strain rate, thus document both the flow field and the magnitude of competency contrast. © 2002 Elsevier Science Ltd. All rights reserved.

Keywords: Competency contrast; Kinematics; Foliations; Lineations

1. Introduction

> "Theories of stress and strain and the concepts of rheology apply essentially to homogeneous continua. Tectonites, although statistically homogeneous, are structurally discontinuous… In setting up a realistic model of rheologic behavior applicable to the interpretation of tectonite fabrics we must take these discontinuities into account, and we must recognize that the rheologic states of the component domains may be very different" Turner and Weiss (1963)

Previous studies of fabric development have been founded on the concept that the orientations of foliations and lineations are sensitive to stress, strain, and kinematic history, although the relative importance of each factor has been debated (e.g. see reviews by Turner and Weiss (1963), Means (1977), Williams (1977), and Passchier and Trouw (1996, p. 57–95)). In general, workers interested in fabric formation have focused on how deformation mechanisms, such as mechanical rotation and dynamic recrystallization, record these factors and thereby contribute to fabric development. By extension, such variables as mineralogy, grain size, temperature, confining pressure, fluid activity, and pore fluid pressure are important in that they control the deformation mechanisms operating in a given shear zone.

Where weak materials, such as micas, are segregated into compositional bands, further fabric development is strongly influenced by strain partitioning between competent and incompetent domains in the rock (e.g. Lister and Williams, 1983; Bell et al., 1986; Williams, 1990). For example, micas segregated in foliation planes have a weakening effect that is disproportionate to their modal volume (e.g. Shea and Kronenberg, 1993; Wintsch et al., 1995). Foliations defined by mineralogically distinct lenses or layers are common in naturally deformed rocks. Examples in fully lithified rock include schistosity, gneissic foliation, most mylonitic foliations, and even slaty cleavage (within which compositional domains are only microscopically visible but are nevertheless key to defining foliation planes; cf. Means

* Corresponding author. Tel.: +1-505-835-5178; fax: +1-505-835-6436.
E-mail addresses: lgoodwin@nmt.edu (L.B. Goodwin), basil@geology.wisc.edu (B. Tikoff).

PII: S0191-8141(01)00092-X

and Williams, 1972). Foliations in faults in sediments can also be defined by compositional domains (e.g. Agar et al., 1989; Heynekamp et al., 1999). The common occurrence of compositional banding in deformed rocks, and evidence that banding facilitates deformation, emphasize the fact that such foliation is mechanically favorable.

DeVore (1969) demonstrated that the development of banding parallel to the maximum principal shear stress during recrystallization of a rock minimizes the mechanical potential energy, but not the chemical potential energy, of the system. Thus, a mechanically stable, compositionally banded rock will include a greater-than-random number of contacts between like grains, even though such contacts have a higher interfacial energy than contacts between unlike grains (Flinn, 1969). DeVore's (1969) conceptual model of fabric development requires diffusive mass transfer to produce banding (that is, to change the distribution of phases to create mechanical equilibrium). Processes of diffusive mass transfer have been emphasized by most researchers investigating the development of compositional banding in both rock (e.g. Cosgrove, 1976; Gray and Durney, 1979; Williams, 1990) and unlithified and poorly lithified sediments (e.g. Agar et al., 1989). Other workers have proposed that the mechanical segregation of phases, and resulting deformation partitioning, may facilitate metamorphic differentiation through solution/precipitation processes in wet rocks (e.g. Means and Williams, 1972, 1974; Williams, 1990). Vernon (1974), however, noted that compositional banding may occur without diffusive mass transfer or 'metamorphic differentiation': if the protolith to a blastomylonite was polymineralic and had a larger grain size than the end-product mylonite, compositional banding could develop simply by dynamic recrystallization of initially large grains.

In this contribution, we describe foliations defined by compositional bands and a sand lineation developed in poorly lithified sediment through particulate flow. These structures formed by mechanical processes only, indicating that processes such as diffusive mass transfer and recrystallization may facilitate, but are not required for, foliation development. The analysis presented in this paper is founded in the assumption that the similarity of foliation patterns developed at all crustal levels reflects a fundamental similarity in the controls on foliation development. We therefore propose a mechanism for development of compositional banding that involves the kinematics and mechanics of a deforming system, but does not require chemical processes of mineral segregation. We suggest that the deformation of heterogeneous geologic media, in which flow is inherently non-steady and locally discontinuous (Jiang, 1994a,b; Jiang and White, 1995), leads inevitably to the mechanical segregation of weaker material into compositional bands, regardless of the specific deformation mechanisms that accommodate flow. We subsequently explore the consequences of this segregation in three-dimensional flow. This leads us to conclude that polymineralic materials have a greater potential for recording all aspects of the flow field, as domains of different competence may, depending on the magnitude of competency contrast, record different deformation paths, and thus different parts of the flow field.

2. Development of compositional banding in granular media

Foliations have been described in natural fault gouges (e.g. Rutter et al., 1986; Agar et al., 1989; Kanaori et al., 1991; Brandon et al., 1994; Lohr et al., 1999), experimentally deformed synthetic fault gouges (see review by Logan et al. (1992), and references therein), and fault zones in unlithified and poorly lithified sediment (e.g. Knipe, 1986; Agar et al., 1989; Heynekamp et al., 1999; Moore et al., 1986; Labaume et al., 1997; Maltman et al., 1997). Foliated cataclasite is particularly evident in faults that cut host rock rich in biotite, and the foliation is defined in part by aligned micas (Chester et al., 1985; Evans, 1988). In incohesive fault gouge or sediments, foliations are typically defined by aligned clays (e.g. Agar et al., 1989; Labaume et al., 1997). Thus, a grain-shape preferred orientation, particularly of layer silicates, is a feature common to many of these foliations. This may indicate either that mechanical rotation accomplished by particulate flow was an important deformation process during foliation development (e.g. Borradaile, 1981), or that grains were crystallizing or recrystallizing in a preferred orientation (e.g. Wintsch et al., 1995).

Of particular interest to this study are foliations defined by compositional banding at both the macroscopic and microscopic scale. Compositional banding has been noted in foliated cataclasite (e.g. Kanaori et al., 1991), incohesive fault gouge (e.g. Lohr et al., 1999), and poorly lithified sediment (e.g. Heynekamp et al., 1999). Bands that record both coaxial and non-coaxial deformation have been described. For example, Agar et al. (1989) documented a single foliation defined by microscopically visible bands developed through coaxial deformation. A foliation defined by banding oblique to the direction of shear, in the orientation of *S*-surfaces in deeper crustal shear zones, has been described in foliated cataclasite (Kanaori et al., 1991), clay-bearing fault gouge (Rutter et al., 1986), and fault zones in poorly lithified sediment (Heynekamp et al., 1999). Rutter et al. (1986) also described compositional foliation banding in the orientations of *C*-surfaces and shear bands (cf. White et al., 1980; Gapais and White, 1982; extensional crenulation cleavages of Platt (1979) and Platt and Vissers (1980); C' foliation of Ponce de Leon and Choukroune (1980)). Such banding can be produced by processes including diffusive mass transfer under low-grade metamorphic or diagenetic conditions (Rutter et al., 1986; Agar et al., 1989) and attenuation of beds through particulate flow in poorly lithified sediments (Heynekamp et al., 1999; G.C. Rawling

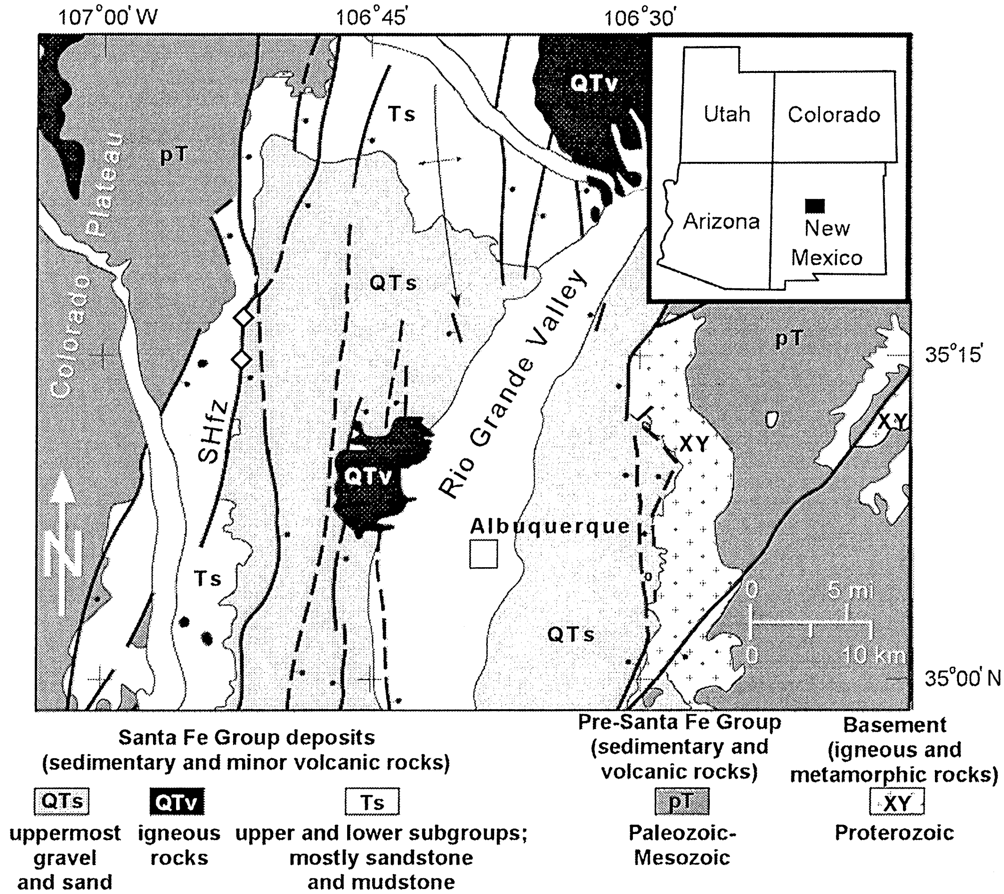

Fig. 1. Study sites (open diamonds: north, Waterfall site; south, Shooting Gallery) along Sand Hill fault zone (SHfz) in Albuquerque Basin, Rio Grande rift. Inset shows location of map. Faults are generalized, and not all faults are shown. Modified from Hawley et al. (1995) and Hawley (1996) by S. Connell.

and L.B. Goodwin, unpublished data). We use the terms *C*-surface and shear band to refer to shear foliations that are essentially parallel or inclined, respectively, to the shear-zone boundaries. Jiang and White (1995) discuss the limitations of this terminology.

2.1. The Sand Hill fault, NM: fabric formed during particulate flow

We describe structures in the Sand Hill fault zone of New Mexico (Fig. 1). The Sand Hill fault is a normal growth fault that cuts poorly lithified sediments of the Santa Fe Group; displacement increases down dip from ~10 to 600 m (Hawley et al., 1995; Heynekamp et al., 1999). At the outcrops of interest, throw is roughly 200 m (Tedford and Barghoorn, 1999); this means that structures have developed in the footwall over the course of 600 m of displacement, whereas hanging wall sediments have seen only 200 m of displacement. The sediments that host the fault were deposited during development of the Rio Grande rift. They are dominantly sand, but include silty sand, silt, mud, and rare gravel. The sands typically have porosities on the order of 30%. Quartz grains generally make up 20–50% or less of the solid fraction of the sands, and the remainder is largely feldspar and lithic fragments. Although they are locally well cemented, the majority of these sediments are so poorly lithified that they can be disaggregated by hand. Stratigraphic constraints indicate that footwall sediments have been buried 190–1050 m (Connell et al., 1999; Tedford and Barghoorn, 1999; S. Connell, written comm., 2001), consistent with vitrinite reflectance data that indicate a maximum depth of burial of 1000 m (W. Shea, pers. comm., 1998). The Sand Hill fault-zone architecture has been described by Mozley and Goodwin (1995), Heynekamp et al. (1999), and Rawling et al. (2001). We summarize key points of this work as the context for the following descriptions.

The Sand Hill fault zone includes a series of roughly tabular architectural elements: a clay-rich core flanked by mixed zones, which are bound by damage zones. The core zone accommodated the majority of the slip. The mixed zones were named because sediment from adjacent beds was incorporated and tectonically mixed into the fault zone, producing material such as clay–sand mixtures (Mozley and Goodwin, 1995; Heynekamp et al., 1999; Rawling et al., 2001). The damage zones are dominated by deformation bands rather than fractures. We focus on structures in the mixed and core zones.

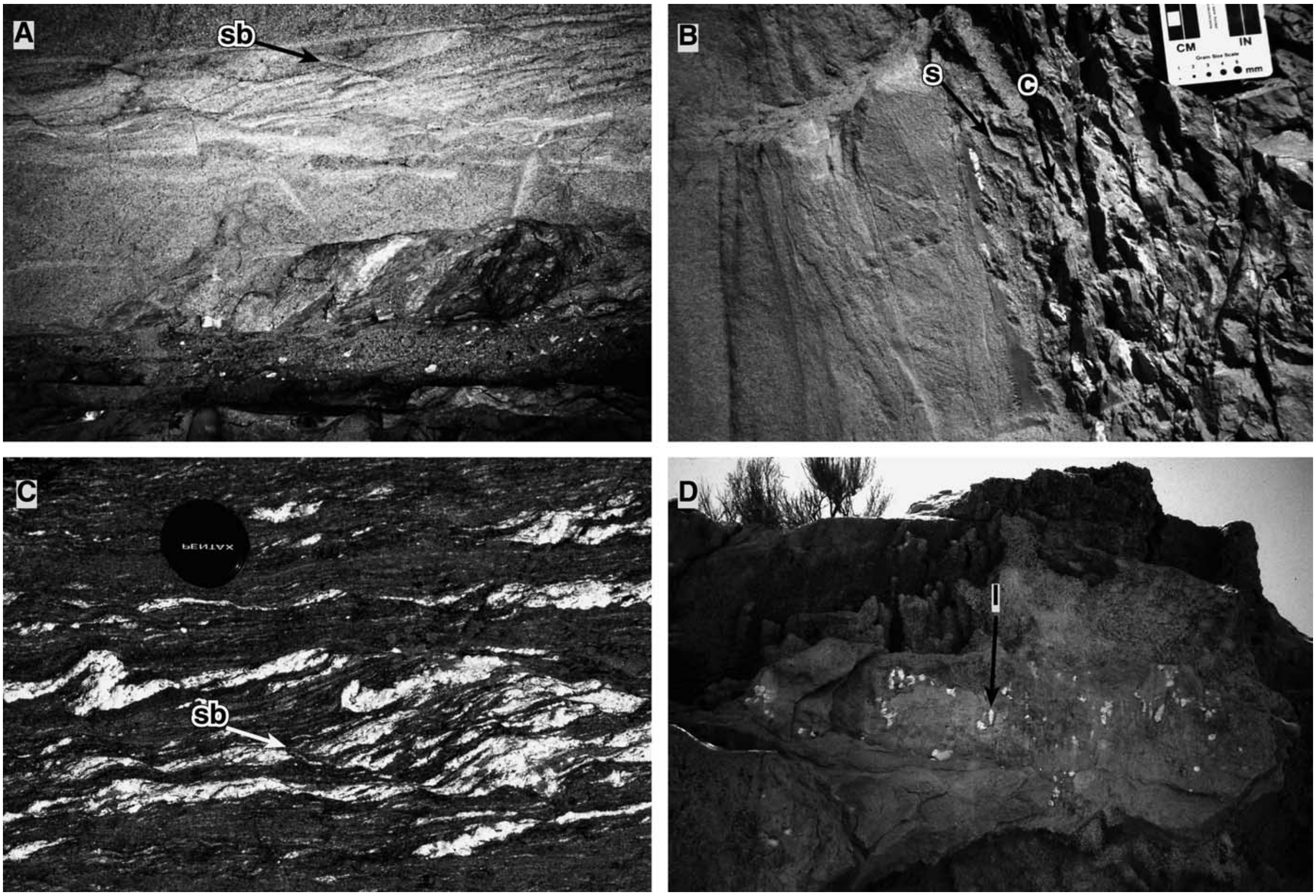

Fig. 2. Field photos of compositional banding foliations. (A) Shear bands (sb) displacing *S*-surfaces in poorly lithified sand; foliations are defined by compositional bands with different grain sizes. Coarser grained sand (darker in color) is segregated along shear bands. Sand Hill fault is an east-side-down (dextral in this image) normal fault; image has been rotated for comparison with (C). Dessication cracks are locally evident. Average size forefinger for scale at base of image. (B) Sand Hill fault zone where it juxtaposes sand against clay, silt, and silty sand. Clay is localized along *S*- and *C*-surfaces (labeled) in poorly lithified clay–sand mixture in fault core; structures viewed to north, recording east-side down shear. (C) Shear bands (sb) in garnet–biotite schist, north coast of Newfoundland. View is of subhorizontal surface; foliation is nearly vertical and transport lineation is subhorizontal. Image has been inverted for comparison with (A). In this view, sher bands and asymmetric folds and boudins show dextral strike-slip shear. Note segregation of biotite along shear bands. Lens cap for scale. (D) Looking south at margin of hanging wall mixed zone of the Sand Hill fault, where it abuts the fault core. Mechanically rotated and extended caliche intraclasts (white) and slickenside striae define a steeply north-plunging lineation (*l*). Elongate concretions behind the slickenside surface are flow features that record the orientation of fluid flow in the fault zone at the time of cementation (Mozley and Goodwin, 1995).

Heynekamp et al. (1999) documented evidence that relict sedimentary structures are locally present in the mixed zones, but that bedding is generally strongly attenuated and disaggregated. The most deformed regions of the mixed zones are well foliated with a grain-shape preferred orientation (Heynekamp et al., 1999; Rawling et al., 2001). Clay–sand mixtures exhibit a foliation defined by aligned clay (Heynekamp et al., 1999). Clay typically surrounds all sand grains in a mixture, and the foliation generally anastamoses around the sand grains. The fault core is also strongly foliated, although bedding is not distinguishable. Petrographic analysis suggests that deformation in both the mixed and core zones was accomplished mainly by particulate flow with subordinate cataclasis (independent particulate flow of Borradaile (1981)); cataclasis within deformation bands is more extensive (controlled particulate flow of Borradaile (1981), Heynekamp et al. (1999) and G.C. Rawling and L.B. Goodwin, unpublished data).

Heynekamp et al. (1999) and Rawling et al. (2001) noted meter-scale *S*- and *C*-surfaces within the footwall mixed zone of the Sand Hill fault. *S*-surfaces are compositional bands defined by attenuated, transposed sedimentary beds are generally inclined to, but curve into, the boundaries of the mixed zone where it meets the fault core and damage zone. *S*- and *C*-surfaces that are not defined by compositional bands are evident at the centimeter scale within the clay-rich core and strongly deformed, clay-rich regions of the mixed zones, where they commonly resemble 'scaly fabric' (cf. Moore et al., 1986). In these cases, striae are generally found on foliation surfaces, and the fault-zone material typically breaks apart along foliation surfaces.

We report on recent observations of centimeter-scale

S-surfaces, *C*-surfaces, and shear bands that are defined by compositional bands. The observations were made in an excavated cross-section of the Sand Hill fault at the Shooting Gallery site (Fig. 1). In the first example, a package of sand is bound to the west and east by fault-parallel shear zones (*C*-surfaces) a few millimeters wide in the hanging wall mixed zone (Fig. 2a). We refer to these as *C*-surfaces because of their orientation parallel to the main fault and evidence for localized shear. The sand package is dominated by a foliation that is oblique to the main fault surface, defined by domains of sand of varying grain size. This foliation is identical, though smaller in scale, to *S*-surfaces described by Heynekamp et al. (1999). Shear bands are locally developed within the package bound by *C*-surfaces. The *S*-surfaces are deflected across the shear bands, and coarse-grained sand is localized within them.

The second example is of *S*- and *C*-surfaces developed locally in the fault core. The core zone is generally clay or sandy clay, but locally includes mesoscopically distinguishable domains of sand. In the location shown in Fig. 2b, *S*-surfaces within the core are defined by segregations of clay in sand. The clay segregations extend from the clay-rich eastern margin of the core zone. The *S*-surfaces are deflected into zones of localized shear along the margins of the core, which we interpret as *C*-surfaces.

Chemical diagenesis and alteration during deformation were minimal in the Sand Hill fault. In the footwall mixed zone, diagenesis is confined to local growth of euhedral zeolite crystals in pores, illitic clay coatings on sand grains, and rare, poorly developed calcite cements (Heynekamp et al., 1999). The core is similarly typically uncemented. In contrast, where the hanging wall mixed zone is coarse-grained, it is well cemented with sparry calcite; where it is fine-grained, it is poorly cemented with micritic cement (Heynekamp et al., 1999). Evidence for processes of diffusive mass transfer in the footwall mixed zone is confined to a single sample, within which subhorizontal solution seams are interpreted as resulting from compaction due to the overlying sediment load. These seams were sheared within synthetic, fault-parallel zones. There is no evidence for solution of sand grains along the foliation in the clay–sand mixtures. Evidence for penetrative particulate flow, however, includes grain and pore alignment within the fault zone and thinning of sedimentary beds (Heynekamp et al., 1999; Rawling and Goodwin, unpublished data).

2.2. Sand lineation

As mentioned above, parts of the Sand Hill fault are well cemented. The process of cementation did not begin until the mixed and core zones had developed (Mozley and Goodwin, 1995; Heynekamp et al., 1999). A variety of geologic data indicate that subsequent to cementation, deformation was localized in the weaker core and footwall mixed zone (Heynekamp et al., 1999). Consequently, the cemented zones preserve structures developed prior to cementation. The well cemented portions of the hanging wall mixed zone are relatively resistant to weathering in comparison to the surrounding poorly lithified sediment, and therefore stand up like a wall. On the surface of the wall that forms the margin between the core and mixed zones, one can see extended pebbles and caliche intraclasts, which define a down-dip lineation (Fig. 2d). Steeply plunging slickenside striae are also locally preserved (Heynekamp et al., 1999). Where the hanging wall sediment is sandy, it is commonly well foliated directly adjacent to the core zone, with a foliation that appears to be fault-parallel and a locally evident lineation apparently defined by sand grains. The sand lineation, like the slickenside striae and extended pebbles, generally plunges roughly down-dip.

A sample of foliated sand was chosen from the hanging wall mixed zone adjacent to the core at the Waterfall site (Fig. 1) for detailed fabric analysis. Three mutually perpendicular sections were cut from the sample (Fig. 3). Section A is perpendicular to the fault and parallel to lineations defined by the long axes of mesoscopically visible sand grains and partially eroded slickenside striae, which appear to be essentially parallel and pitch 83°N on the fault plane. Section B is perpendicular to the fault and the inferred slip direction, and section C is parallel to the fault plane. Maps of each thin section were constructed from enlargements made on a microfiche reader. A series of reference lines was drawn on each map, and the long and short axes and angle between the long axis and reference line were measured for grains that intersected the reference lines at regular intervals. The lines were drawn parallel to either the fault margins or mesoscopically visible lineations, allowing the geologic significance of any preferred orientation to be assessed. Two hundred grains from each section were analyzed. After eliminating data collected from grains with axial ratios less than 1.4 (following Shelley (1995) and Cladouhos (1999), who showed that the orientations of grains with low aspect axial ratios could not be reliably measured), 115–138 measurements remained for each section (Fig. 3).

These data demonstrate that the foliation and lineation visible in outcrop are defined by the aligned long axes of sand grains. The mean orientations of the long axes of sand grains are inclined to both the slip direction and fault surface by less than 6.5°. Because it is unlikely that the orientations of thin sections with respect to fault coordinates are more accurate than ±5–10°, these inclinations are not considered significant. However, the symmetry of the grain orientation distribution should not be affected by errors in orientation. All sections exhibit some asymmetry, which is particularly pronounced in the section cut parallel to the slip direction and perpendicular to the fault (section A). The latter indicates that a significant number of grains are oriented roughly parallel to the fault, but a larger number of grains are inclined to the fault in an *S*-surface orientation. The

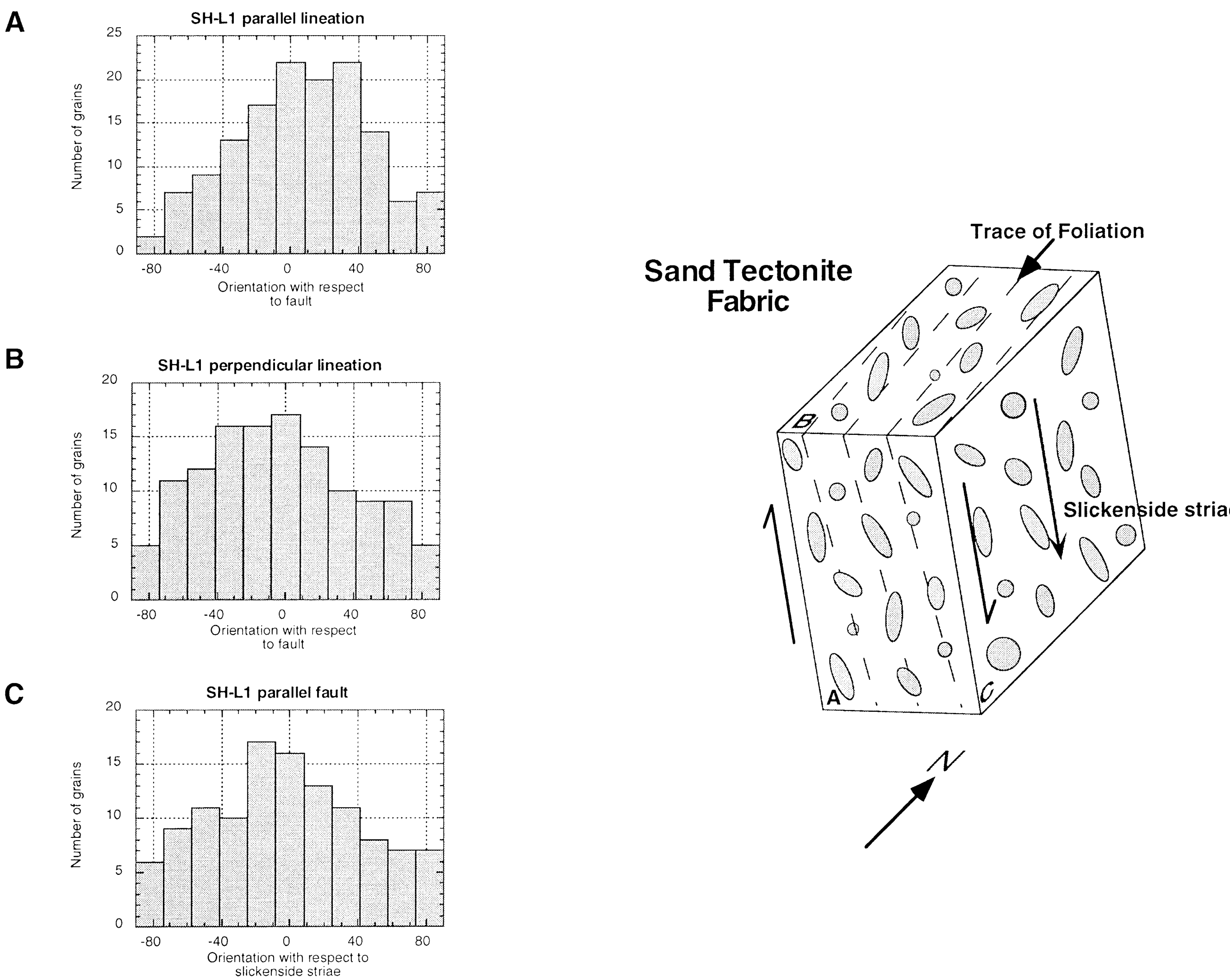

Fig. 3. Grain alignment in sand tectonite. (A)–(C) show histograms illustrating orientations of long axes of sand grains with axial ratios $\geqq 1.4$ relative to trace of fault (A and B) or slip direction (C). Histograms correspond to labeled faces of cartoon (right) showing fabric; (+) angles represent counterclockwise orientations, (−) angles are clockwise from reference line. (A) Section cut parallel to lineation, perpendicular to fault, viewed in orientation shown in block diagram. (B) Section cut perpendicular to fault and slip direction, viewed looking up dip. (C) Section cut parallel to fault, viewed looking east.

asymmetry evident in other sections may indicate that they were cut oblique to the main structures, or that the symmetry of the tectonite as a whole is triclinic rather than monoclinic. Discrete foliation planes in multiple orientations are not evident in either outcrop or thin section. The lineation is essentially parallel to the inferred slip direction, recorded by slickenside striae at the margin between the mixed and core zones.

The sand fabric is generalized in a cartoon in Fig. 3. The aspect ratios of grains viewed in each of the three mutually perpendicular directions are different. The variations in aspect ratio are consistent with the alignment of elliptical grains such that the shortest axis is perpendicular to the foliation and the longest axis is subparallel to the transport direction defined by slickenside striae. We propose that this fabric developed largely through the mechanical rotation of sand grains during particulate flow.

2.3. Discussion

The purpose of describing structures developed by independent particulate flow is twofold. (1) It emphasizes the point that because similar structures are found in shear zones in a variety of rocks and sediments deformed over a wide range of physical conditions, the processes of foliation formation cannot depend fundamentally on a specific deformation mechanism or combination of mechanisms (Rutter et al., 1986). (2) It suggests that the most fundamental controls on development of foliation defined by bands are probably mechanical, as chemical processes are not required to produce compositional banding.

Fabrics similar to those we have shown developed in the Sand Hill fault zone are found throughout the crust, from near-surface environments such as the latter to granulite facies shear zones (e.g. Hanmer et al., 1995). Examples of

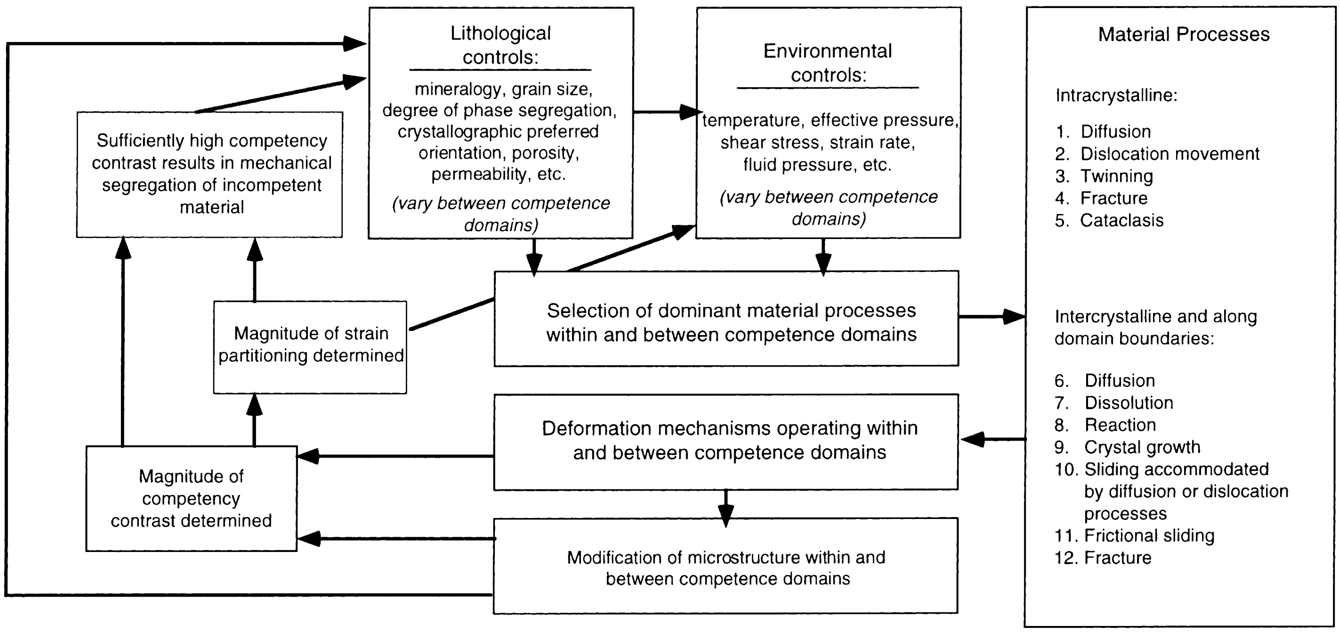

Fig. 4. Flow chart showing the variables affecting the behavior of deforming earth materials and the relationship between deformation mechanisms and competency contrast. Note the importance of deformation mechanisms operating both within and between competence domains. Modified from Knipe (1989).

compositional banding fabrics with monoclinic symmetry in greenschist to amphibolite facies shear zones are too numerous to list; since the earliest description of *S*- and *C*-surfaces and shear bands (Berthé et al., 1979; Platt, 1979), many occurrences have been documented. A characteristic of these structures is the segregation of mechanically weak or incompetent phases along shear surfaces. Fig. 2c, for example, is a field photo of rocks exposed on the west coast of Ragged Harbour, along the boundary between the Gander and Dunnage zones in northern Newfoundland, which record strike-slip shear under amphibolite facies conditions (Goodwin and O'Neill, 1991). The foliations in this area are defined by mineralogical domains and the preferred dimensional alignment of biotite and polycrystalline aggregates of other phases. Biotite is localized along *S*-surfaces, *C*-surfaces, and a well developed shear-band foliation. As mentioned earlier, the segregation of biotite, the rheologically weakest phase in the rock, into foliation planes is a common observation in fault zones as well as greenschist and amphibolite facies ductile shear zones. It is analogous to the localization of clays in *S*-surfaces in shallow crustal faults (e.g. Fig. 2b). Even in fault-zone materials with little to no clay, segregation of the weakest material is evident (Fig. 2a). Coarse-grained sand, localized along shear bands in sand, has greater porosity and fewer grain–grain contacts than fine-grained sand, and so is weaker where frictional deformation mechanisms are dominant. Thus, the development of compositional bands at all crustal levels appears to involve the segregation of incompetent material into foliations.

Rocks deformed under granulite facies conditions also locally exhibit multiple foliations, such as *C*-surfaces and shear bands, but are distinct from the above examples in that they generally exhibit only a single mesoscopically visible foliation. We have, for example, observed shear bands in granulite facies rocks from the Arunta block in central Australia, but they are rare. Foliations oblique to the main compositional layering may be microscopically evident within mineralogical domains (e.g. White and Mawer, 1992), but multiple foliations defined by compositional layers are not typical of granulites. The more common granulite fabrics, which appear orthorhombic in the field, may reflect either low mechanical contrast between phases at high homologous temperature (discussed in the following section), high strain (J. White, pers. comm., 2001), or a preponderance of coaxial deformation at deeper crustal conditions.

The deformation mechanisms by which foliations form at the very different crustal levels discussed above are obviously very different. They range from frictional grain-boundary sliding and particulate flow in the Sand Hill fault zone to crystal plastic flow and recrystallization in deeper crustal shear zones. The common factor in each of these examples, however, is the segregation of the rheologically weakest, or least competent, phase into bands. We thus begin our exploration of the mechanisms of phase segregation with a discussion of competency contrast.

2.3.1. Competency contrast

The terms 'competence' and 'competency contrast' have been used by a variety of authors over the years to describe qualitatively the relative mechanical behavior of different domains in a deforming material (for the earliest definitions, see Willis (1893), van Hise (1896), and Dennis (1967)). Informative discussions of the rheological significance of competency contrast are offered by Lister and Williams (1983) and Jiang (1994b), who point out the kinematic consequences of mechanical variations in rocks. In this paper, we focus on one aspect of what has been referred to as competency contrast: differences in deformation behavior between adjacent domains, which fundamentally reflect mechanical contrast. We use the broad term 'mechanical' deliberately, to include the variation from frictional grain-boundary sliding in fault-zone materials to crystal–plastic flow and diffusion-dominated processes in deep crustal shear zones.

In this paper, we refer to volumes of a deforming material that are mechanically distinct from other volumes as competence domains. It is important to note that competence is not just a property of a given domain under a given set of physical conditions, but depends in part on the mechanical behavior of adjacent domains (Turner and Weiss, 1963). For example, progressive partitioning of deformation into incompetent domains will increase the strain rate in the incompetent domains relative to more competent domains (Fig. 4). These variations in strain rate may be sufficient to affect the deformation mechanisms operating in individual domains. In addition, the mechanisms by which deformation is accommodated in adjacent domains can influence the deformation mechanisms at domain boundaries. Thus, the magnitude of competency contrast within a deforming body will change as such variables as temperature, confining pressure, pore fluid pressure and composition, strain rate, and stress orientation and magnitude change and impact the deformation mechanisms operating within and between both competent and incompetent domains. A feedback loop therefore exists between competency contrast and deformation mechanisms, as the magnitude of competency contrast will also influence the above variables (Fig. 4).

Competence domains have a variety of characteristics, as follows:

1. Domains of a given mineral may or may not have the same competence. Fine-grained material will generally exhibit different mechanical behavior than coarse-grained material, and therefore mineralogy alone does not define competence domains (e.g. Tullis and Yund, 1985).
2. Competence domains may or may not be monomineralic. More or less competent domains may reflect either the distribution and/or percentage of mineral phases in different domains, or simply variations in grain size. Domains that vary only in grain size may or may not have different competence, depending on whether or not the grain-size variation is sufficient to affect the deformation behavior in a given system (e.g. Etheridge and Wilkie, 1979; White, 1982; Tullis and Yund, 1985; Goodwin and Wenk, 1995).
3. The competence of a given domain will depend in part on its orientation, and the orientation of constituent grains, with respect to imposed stress or displacement. For example, Donath (1961) demonstrated that a slate loaded perpendicular to its foliation was very strong, whereas the same rock loaded at a low angle to the foliation was very weak. Deformation of a quartzite mylonite produced similar results (Ralser et al., 1991).
4. Pore space can be considered a 'phase' for the purpose of evaluating competency contrast (cf. Handy, 1990). Consequently, unlithified material that contains only one mineral phase (i.e. quartz sand) will nonetheless behave as a polyphase material by virtue of porosity and therefore contains a competency contrast.
5. Monomineralic rocks, even those that are equigranular, can also contain competency contrasts. As noted by Law et al. (1986), quartz grains can be oriented such that their slip systems are well aligned for flow (soft grains) and others may be poorly aligned (hard grains). As a consequence, competency contrast is created by variations in the orientation of the potential slip systems.
6. A given competence domain will be characterized during deformation by a vorticity number that may be temporally variable, but will be distinct from that of domains of different competence (Jiang, 1994a).

The relationship between strength and composition of polymineralic materials is highly nonlinear. Handy (1990) defined three end-member mechanical and microstructural types of polymineralic rocks: (1) a competent phase(s) forms a load-bearing framework around physically isolated incompetent phase(s); (2) two or more relatively incompetent minerals control bulk rheology, and form elongate boudins; and (3) competent minerals form clasts in an incompetent matrix, which controls the bulk rheology.

As evident from the above summary, the relative volume percent, orientation, and distribution of competent and incompetent phases in a deforming material will influence competency contrast. It follows directly that syntectonic changes in these variables will impact competence and competency contrast. Such changes can occur during deformation by: (1) reaction weakening or hardening (e.g. White and Knipe, 1978; Etheridge and Wilkie, 1979; Knipe and Wintsch, 1985; Wintsch, 1985; O'Hara, 1988; Wibberly, 1999); (2) reorientation of grains during crystal–plastic flow, which can cause geometrical softening (e.g. White et al., 1980; Lister and Williams, 1983) or hardening (e.g. Takeshita and Wenk, 1988); (3) chemical segregation processes (e.g. Cosgrove, 1976; Gray and Durney, 1979; Williams, 1990); and (4) grain-size reduction and redistribution of phases during cataclasis or pseudotachylyte formation (e.g. Goodwin and Wenk, 1995; Goodwin, 1999).

One could argue that all earth materials have some competency contrast; however, cases in which the competency contrast is minimized can be envisioned. For example, certain minerals, such as quartz and feldspar, exhibit different strengths at most temperature, pressure and strain-rate conditions, but at specific conditions can exhibit a similar strength (Tullis, 1990), so that competency contrast could be minimized under specific environmental conditions for a given deforming material. The difference in rheology between minerals in a given rock will, however, generally decrease as they reach higher homologous temperatures; that is, competency contrast will decrease (e.g. Passchier and Trouw, 1996, p. 106). This decrease in competency contrast is a result of the increased efficiency of solid-state diffusive mass transfer and crystal–plastic deformation mechanisms, and a decrease in differential stress at higher metamorphic grade. Passchier and Trouw (1996) suggest that this will result in a relatively coarse-grained rock with a single foliation, well defined by compositional bands, such as that exhibited by many granulites. Perhaps the material with the least possible contrast, however, would be a monomineralic rock deformed to high strains through dislocation creep, so that the bulk-rock crystallographic preferred orientation (CPO) approached that of a single crystal. Thus, strain magnitude must also influence competency contrast.

3. Material heterogeneity, compositional banding, and flow partitioning

The domainal character of earth materials indicates that they need not be flowing continuous media at the scale of competence domains. At the scale of domains of interest, they exhibit a range of mechanical behavior between true continua (where domain boundaries behave as coherent interfaces; cf. Cobbold, 1983) and true granular media (where coupling across domain boundaries is not expected). This range in behavior encompasses Borradaile's (1981) categories of particulate flow, which include dependent, controlled, and independent particulate flow, in order of increasing importance of grain-boundary sliding and decreasing importance of intragranular deformation processes.

The physics of granular flow is poorly understood, but in general it can be stated that true granular media, such as the deformed sediment illustrated in Fig. 1, cannot be modeled as either solid or fluid (e.g. Shinbrot and Muzzio, 2000). A relevant non-geologic case is that of grain stored in silos (Behringer's Nonlinear Flow Group, 2001). The initial practice of engineering silo design to accommodate a fluid of equal volume to the grain to be stored was abandoned following silo failure. Shear zones developed in the grain-pore system in response to the vertical load of grain, and propagated through the walls of the silo. We suggest that this organization of a grain-pore system into shear zones in response to imposed displacement or stresses may well be analogous to the development of localized shear zones in earth materials. If this analogy is appropriate, it suggests that the domainal character of heterogeneous earth materials is a fundamental control on the localization of strain in shear zones as well as on the fabrics that are produced by shear.

The range in deformation behavior exhibited by natural materials reflects their heterogeneity and thus competency contrast. In the following sections, we draw on the results of previous deformation experiments to emphasize the role of competency contrast in determining whether or not compositional banding is produced in deforming earth materials.

3.1. Development of compositional banding: experimental deformation of initially isotropic synthetic rock

Experiments provide special insight into deformation processes because temperature, pressure, and strain rate can be controlled during deformation. In addition, it is possible to stop the experiments at different stages and thereby investigate the development of structures with increasing strain. A particularly relevant experimental study by Jordan (1987) focused on the development of foliation defined by compositional bands in nonfoliated synthetic rocks. The description of these experiments and results, below, are followed by our interpretation of their significance and a proposed mechanism for mechanical segregation of phases.

Jordan (1987) subjected aggregates of limestone and halite to both coaxial and non-coaxial deformation. For the axially symmetric compression experiments we discuss here, deformation took place at room temperature, 150 MPa confining pressure (P_c), and a strain rate of 10^{-4} s^{-1}. Non-coaxial experiments were conducted at room temperature, 250 MPa P_c, and a shear strain rate of 10^{-4} s^{-1}. Under these conditions, the halite deformed through crystal–plastic flow, whereas the behavior of the Solnhofen limestone was transitional between cataclastic and crystal–plastic flow (deformation by twinning). Monomineralic deformation experiments indicated that the flow strength of the less competent halite was roughly an order of magnitude less than that of the more competent limestone.

Results of key experiments are reproduced in Fig. 5, with Fig. 5a–d showing the evolution of the coaxial experiments and Fig. 5e showing the result of a non-coaxial experiment. Both sets of experiments produced a foliation defined by bands of halite (dark) and calcite (light). The fabric produced through coaxial deformation is symmetrical about the shortening direction, whereas that produced through non-coaxial deformation is asymmetrical. The compositional foliation banding is better developed in the non-coaxially deformed specimens because the experimental set-up allowed deformation to higher strains (Fig. 5e). An important observation is that the samples weakened significantly with increasing foliation development in both coaxial and noncoaxial deformation, such that the bulk strength was lower than expected if the relationship between the relative proportions of calcite and halite and flow strength were linear. This observation is consistent with DeVore's (1969) conclusion that

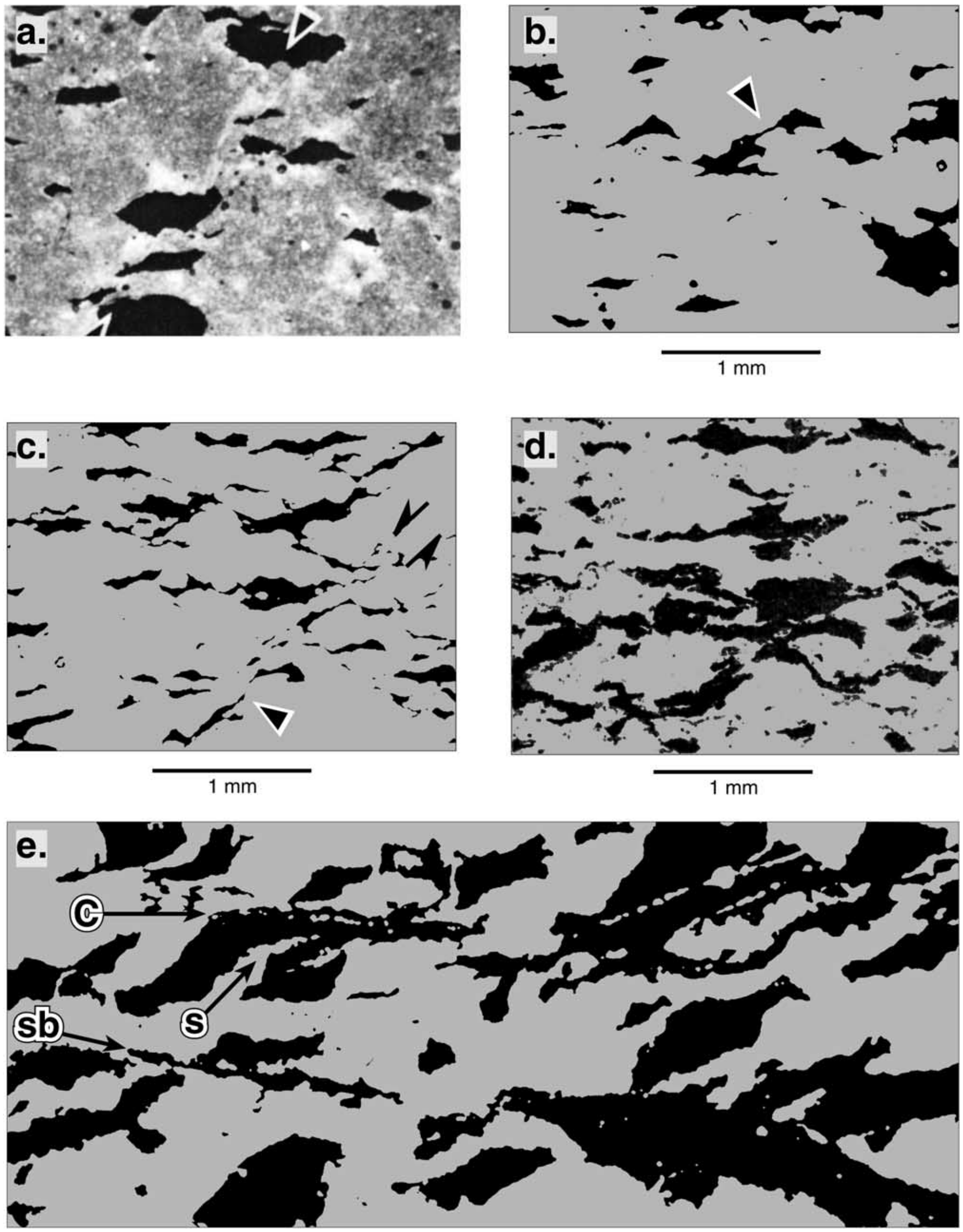

Fig. 5. Summary diagram illustrating development of compositional banding through coaxial (a–d) and non-coaxial (e) deformation of limestone-halite aggregates, after Jordan (1987). Most images have been converted from grayscale to binary to emphasize distribution of halite (black) and calcite (gray). (a) Early stage of deformation, with strains that locally approach 20%. Cataclastic shear zones in limestone have nucleated on margins between halite and limestone (arrow), and locally connect halite domains. Some E–W elongation of halite domains. Shear zones form an angle of ~35° to the shortening direction. Cuspate–lobate domain margins record competency contrast between halite and limestone. Scale the same as b–d. (b) Local strains of ~35% result in segregation of the weaker halite within shear bands (arrow) and rotation of shear bands away from shortening direction. (c) Up to 50% shortening locally. Left-hand side of diagram: initially formed shear bands have rotated to a high angle to the shortening direction. Right-hand side of diagram: halite has further segregated into new shear bands (related to experimental configuration) oriented at 30° to the shortening direction (arrows). (d) 50% shortening with 35% halite. Formation of compositional layering caused by segregation of halite. Note inversion of matrix/clast pattern with respect to (a). (e) Development of multiple foliations through dextral, non-coaxial shear. *S*-surfaces (*S*) initially formed at 45° to the bulk shear plane, then rotated. Shear strain up to 1.6, largely concentrated into *C*-surfaces (*C*) and shear bands (sb). Scale bar is 0.5 mm.

development of compositional banding in a rock will lower its mechanical potential energy.

The formation of banding is best illustrated by the coaxial deformation of samples with 10–20 vol% halite (Fig. 5a–d), although the process is similar in non-coaxial experiments (Jordan, 1987). The starting material consisted of isolated halite domains in a calcite matrix. At low strains, deformation was accommodated by: (1) shortening of halite domains parallel to the imposed load and extension perpendicular to shortening; and (2) nucleation of cataclastic micro-shear zones at competence domain boundaries, and extension of the shear zones into the competent calcite domains, in some cases connecting halite domains (Fig. 5a). The cuspate–lobate morphology of the edges of the flattened halite domains records the competency contrast between halite (cusps) and calcite (lobes). With continued deformation, halite was progressively segregated into conjugate shear zones, or shear bands, causing the previously continuous calcite matrix to be subdivided into separate domains (Fig. 5b and c). The shear bands initiated at ~35° to the shortening direction, then progressively rotated to a sub-horizontal orientation, perpendicular to the shortening direction, forming a distinct compositional foliation banding (Fig. 5d).

Segregation of halite into compositional bands did not occur in the relatively high temperature (200°C) coaxial experiments, and patterns were less distinct with increasing confining pressure. In samples with high halite content, formation of shear bands was also not evident, except where forced by the experimental configuration (i.e. boundary conditions). The foliation in these samples is defined largely by the orientation of grain boundaries perpendicular to the shortening direction.

Samples with ~55% halite deformed in non-coaxial shear resulted in the segregation of phases into compositional bands. The latter experiments resulted in the simultaneous development of *S*- and *C*-surfaces. Deformation was increasingly partitioned into *C*-surfaces with increasing strain, and *S*-surfaces accommodated this partitioning by rotating toward the *C*-surfaces. Both *C*-surfaces and, subsequently, shear bands developed through the formation of cataclastic micro-shear zones, along which halite was subsequently localized. Halite domains were connected through progressive deformation, in a process similar to that described above for coaxial deformation. Jordan (1987) noted that the main shear displacement switched between *C*-surfaces and shear bands, depending on the original distribution of halite domains in the system, and that the two shear planes showed a close genetic relationship. In these experiments, the development of compositional banding in non-coaxially deformed specimens was dependent on the percentage of competent domains in the sample; >20% competent domains was required for shear strain to be localized into bands. Where competent domains were rare or absent, only *S*-surfaces formed.

3.2. Interpretation of Jordan's (1987) data: the significance of competency contrast

Jordan (1987) documented a foliation-weakening process, where progressive segregation of the incompetent phase into a compositional foliation banding was accompanied by progressive partitioning of the deformation into incompetent domains. He suggested that: (1) the mechanical strength of polyphase rocks is controlled by the weakest phase; and (2) that the ultimate strength of a rock will be determined by the deformation mechanisms operating in each phase and their competence, shape, orientation, and distribution. In addition, he suggested that the development of shear bands and *C*-surfaces requires the presence of a critical amount of a stronger phase, and that lacking that critical volume, only *S*-surfaces will form.

In this and the following section, we build on the above conclusions to suggest a mechanism for the development of compositional banding in earth materials in general, and offer an explanation for why shear bands and *C*-surfaces form in systems with competency contrast. The essence of our argument is that high competency contrast leads to the segregation of phases in both coaxial and non-coaxial deformation because of differences in strain and strain rate between adjacent domains. In contrast, the lowest competency contrast experiments do not result in phase segregation.

Halite + calcite samples deformed at room temperature (Fig. 5; Jordan, 1987) correspond to Handy's (1990) mechanical type 1: materials in which the competent domains are connected and load-bearing. High competency contrast in these experiments is recorded by lobate/cuspate domain boundaries. The process of development of compositional bands in these samples was fundamentally the same in either coaxial or non-coaxial deformation. Cataclastic shear bands (and *C*-surfaces in non-coaxial deformation) nucleated at competence domain boundaries and propagated through the competent domains, linking incompetent domains. Halite, the incompetent phase, became progressively segregated into the shear bands with increasing strain. In coaxial shear, conjugate shear bands progressively rotated into an orientation that was ~90° from the shortening direction. The initial configuration of phases, with isolated halite domains surrounded by calcite, was reversed through this process, which produced a network of halite bands surrounding isolated calcite domains in coaxial deformation. Non-coaxial deformation produces an interconnected network of halite localized along *S*-surfaces, *C*-surfaces, and shear bands. Thus, the number and orientation of foliations defined by compositional bands records the deformation path (Fig. 5). Note that the fabric patterns and microstructures record more information in these samples than in samples with low competency contrast, discussed below.

Samples deformed at higher homologous temperatures exhibited lower competency contrast. In halite + calcite samples deformed coaxially at 200°C (Jordan, 1987), the foliation was defined largely by the orientation of grain boundaries perpendicular to the shortening direction. Segregation of halite into compositional bands did not occur. Jordan (1987) suggested that this lack of compositional banding reflects the increasing importance of crystal–plastic deformation mechanisms in the limestone domains with increasing temperature. We alternatively suggest that the lack of banding is the result of a reduction in competency contrast, related to this change in dominant deformation mechanisms. Low competency contrast

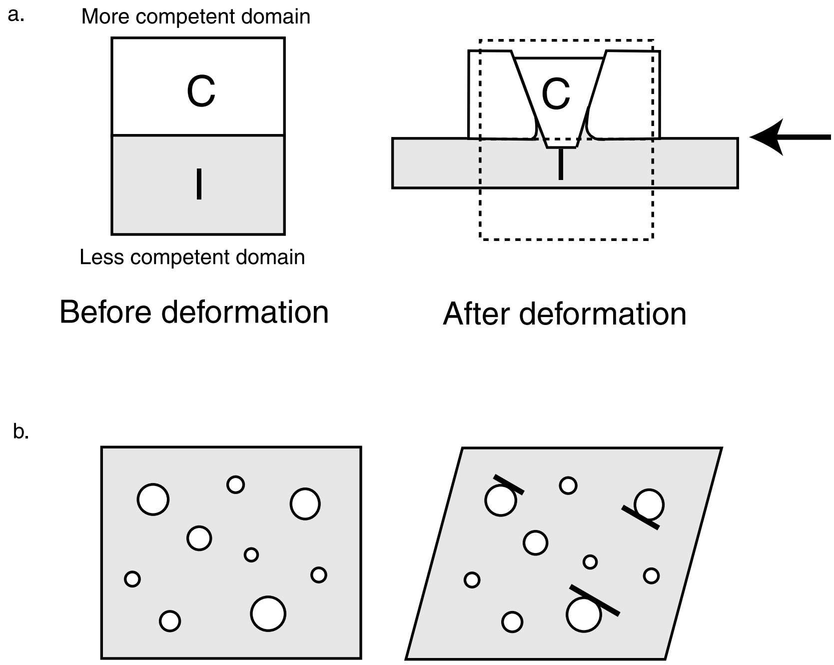

Fig. 6. Scale-independent cartoons of two simple configurations of competent (white) and incompetent (gray) domains subjected to coaxial deformation (a) and dextral simple shear (b). Both strain and strain rate are higher in the incompetent domains than in the competent domains, and strain incompatibility occurs at domain boundaries. (a) Conjugate shear bands nucleate at domain boundary in coaxial deformation. Deformation is more localized in competent domain, providing a mechanism for localization of incompetent material within shear bands. (b) Shear bands (bold lines) nucleate at the margins of the largest porphyroclasts. See text for more detail.

allowed a foliation defined by the preferred dimensional alignment of compositional domains to form, but did not provide a mechanism for segregation of phases into compositional bands. Fabric patterns in Jordan's (1987) experiments were also less distinct in samples deformed at higher confining pressure, which again should have resulted in a decrease in competency contrast.

Jordan (1987) noted that, in non-coaxial deformation, samples with 20% or less calcite (the competent phase) formed *S*-surfaces, but did not develop shear bands or segregation of phases. These samples represent Handy's (1990) type 3 mechanical end-member, in which the incompetent phase controls the bulk rheology of the sample. Because the competent phase occurs as isolated clasts in an incompetent matrix, the bulk rheology is similar to that of a system with low competency contrast.

We propose that deformation of a material with significant competency contrast results in a compositional foliation banding because different competence domains deform at different strain rates and attain different finite strains, producing strain incompatibilities at domain boundaries (Fig. 6). Sufficiently large incompatibilities cannot be accommodated by domain-boundary deformation processes, and thus will produce mechanical instabilities, causing micro-shear zones (shear bands and/or *C*-surfaces) like those produced in Jordan's (1987) experiments to form. Thus, deformation in competent domains is largely localized within shear zones, whereas it is distributed in incompetent domains. The process of formation of compositional bands, and subsequent deformation, is essentially one of strain partitioning. Shear bands and *C*-surfaces experience (at least initially) dominantly non-coaxial deformation, whereas the intervening domains preferentially record shortening at right angles to the applied load. Thus, the more competent domains can deform internally although, as Jordan (1987) pointed out, they may cease to deform if an interconnected network of weak material can accommodate all of the deformation. The character of deformation in the different domains will be recorded by both their internal microstructure and their three-dimensional morphology.

In cases of very low competency contrast, mechanical instabilities do not occur, and therefore there is no formation of shear bands or resultant segregation of phases. Rather, a single foliation defined by a grain-shape preferred orientation forms.

3.3. Initiation of shear bands as a result of competency contrast: a natural example

The physical experiments outlined above suggest that competency contrast is required for the nucleation of shear bands and *C*-surfaces. At first glance, it would not appear that this argument would be generally applicable to all deformed materials. Apparently contradictory examples are shear bands within naturally deformed quartzite mylonites (e.g. Law et al., 1984) and experimentally deformed dunites (Zhang and Karato, 1995), both of which are essentially monomineralic. However, as noted earlier, even monomineralic rocks are mechanically heterogeneous and thus have competence domains, such as those produced by the hard and soft orientations of potential slip systems (e.g. Law et al., 1986). In addition, there are trace phases (such as micas), even in essentially monomineralic rocks, on which to nucleate shear bands. Therefore, we assert that competency contrast is required for localization of deformation. However, natural systems may require significantly less competency contrast or a smaller percentage of a second phase than experimental systems in order to nucleate shear bands.

To investigate the nucleation of shear bands in a natural system, we have chosen an area that exhibits: (1) variation in strain in the absence of variation in rock type; (2) preservation of relatively low strain areas, which we interpret to record the early stages of deformation of the rock, assuming that the shear zone did not widen (cf. Means, 1995); and (3) a protolith with high competency contrast. We focus on the Rosy Finch shear zone in the Sierra Nevada batholith, where it cuts through the center of the Mono Creek pluton (Tikoff and Teyssier, 1994). The Mono Creek pluton is a porphyritic granite, containing quartz, K-feldspar, plagioclase, biotite, and accessory phases. The exposures studied were intruded at shallow depths, corresponding to 100–200 MPa of pressure. Deformation occurred at greenschist facies conditions. Within the dextral, transpressional Rosy Finch shear zone, quartz underwent dominantly crystal–plastic flow, whereas K-feldspar porphyroclasts record minor brittle deformation (e.g. bookshelf-sliding) or are undeformed (e.g. Tikoff and St. Blanquat, 1997). The highest strain is recorded by rocks in the middle of the shear zone, with undeformed granite on both sides. These strain gradients allow one to observe evidence for the initiation of shear bands in the Mono Creek granite.

In low strain areas at the margins of the Rosy Finch shear zone, shear bands have nucleated on the margins of the largest K-feldspar porphyroclasts (Fig. 6b). We interpret these micro-shear zones as the result of a mechanical instability, caused by the competency contrast between the pophryroclasts and the deforming matrix. It is unlikely that the competence of the largest K-feldspar megacrysts differs dramatically from the smallest (clasts range from 3 to 5 mm in size). Therefore it is the size of the porphyroclasts, or competent domains, that causes the localization. Deformation is localized because the porphyroclasts are large, essentially rigid obstacles in the flow field, which requires the strain rate at their edges to increase with increasing clast size. This indicates that the variation in strain rate resulting from the size of the competent domains controlled the formation of the mechanical instability and subsequent nucleation of shear bands.

Shear-band spacing is also controlled by the competent domains. In the middle of the Rosy Finch shear zone in the Mono Creek granite, the rock is dominated by shear bands, which separate 'trains' of imbricated K-feldspar porphyroclasts (Fig. 7a). Consequently, the shear bands have a characteristic spacing — that of the 'average' porphyroclast size. In the middle of the shear zone, the average porphyroclast size is less than the mean size of K-feldspar megacrysts in undeformed parts of the Mono Creek granite, suggesting grain-size reduction through deformation. K-feldspar porphyroclasts in the middle of the shear zone locally escaped significant grain-size reduction. One such example, in Fig. 7a, is a large porphyroclast that disrupted the regular spacing of the foliation surfaces. Thus, variations in shear-band foliation spacing are controlled by variations in the size of the most competent domains (porphyroclasts in this case), which may be related to differences in either strain (degree of deformation-induced grain-size reduction; Fig. 7c) or protolith (initial grain-size variation).

One last interesting effect is the variation in deformation mechanisms with proximity to the large porphyroclasts in both the Mono Creek granite and Lake Edison granodiorite, which is also cut by the Rosy Finch shear zone. Relatively far from the K-feldspar porphyroclasts, quartz and biotite exhibit microstructures that suggest deformation by crystal–plastic flow. However, immediately adjacent to the porphyroclasts, deformation was localized within the narrow zones that define shear bands, on which ridge-in-groove slickenside striae are visible in hand sample. The grain size of both minerals is much smaller in these zones than in regions further from the porphyroclasts. There is evidence of dynamic recrystallization of grains, but micro- and mesostructures suggest that biotite and, locally, quartz may deform in part by frictional grain-boundary sliding on shear bands (Fig. 7b). This variation in dominant deformation mechanisms with distance from competent domain boundaries records variations in strain and strain rate between domains, and thus depends fundamentally on the magnitude of competency contrast.

The K-feldspar porphyroclasts in the Rosy Finch shear zone define the size of competence domains, thus competency contrast occurs at the mesoscopic scale in this example. This emphasizes an important point of our analysis: although we are particularly interested in microstructures, this approach is applicable from the thin-section to the regional scale. It appears that kinematic domains (shear domains of Turner and Weiss (1963); banded deformation structures of Cobbold (1977)) within earth materials are largely controlled by competency contrast.

4. Kinematics and competency contrast: strain and strain-rate partitioning

Fig. 6a illustrates deformation of adjacent competent and incompetent domains. In this scale-independent cartoon, both domains have experienced coaxial deformation, but the strain magnitude is greater and strain rate was higher in the incompetent domain. Thus, the structures that result from competency contrast will record strain rate variations.

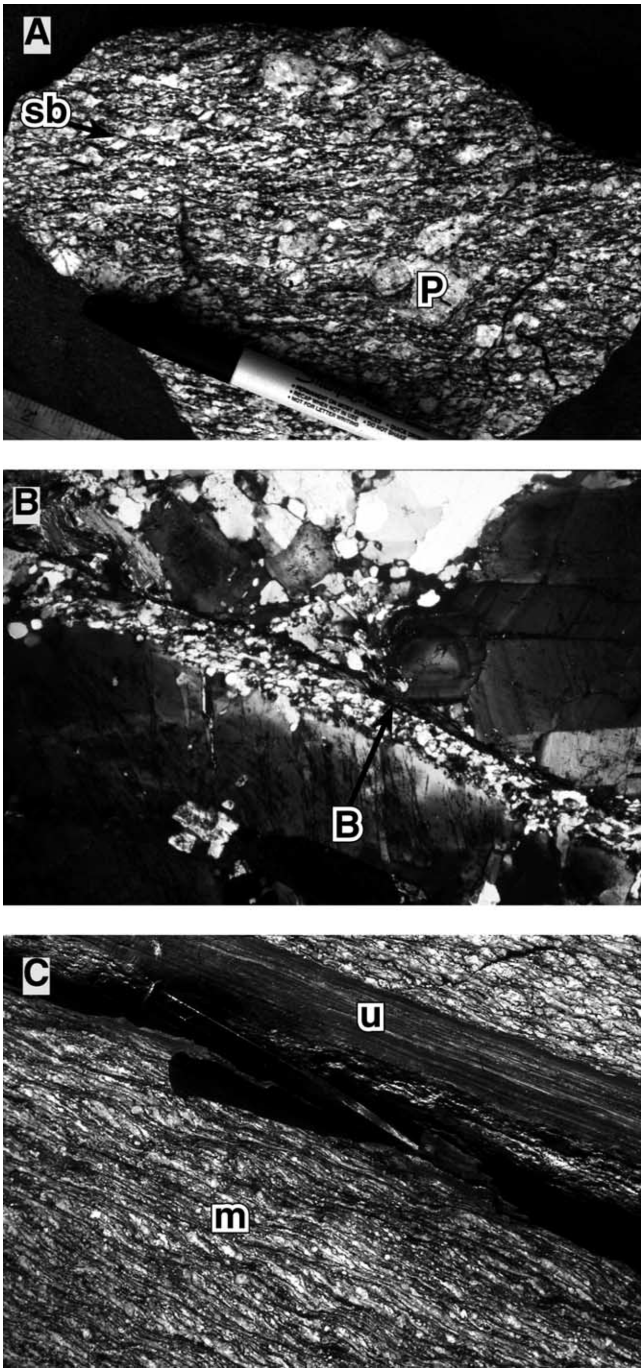

Fig. 7. Examples from the Rosy Finch shear zone, Sierra Nevada batholith, California: (A) Hand sample from the Mono Creek granite, showing the effect of competency contrast on the spacing of shear bands (sb). The size of the feldspar porphyroclasts controls the spacing of shear bands, and particularly large porphyroclasts (e.g. P) disrupt the characteristic spacing. (B) Lake Edison granodiorite. Section cut perpendicular to foliation and parallel to ridge-in-groove slickenside striae. Photo taken with crossed polars; field of view is 3.2 mm wide. A brittle-ductile shear band (B) formed between large feldspar porphyroclasts, which acted as competent domains. Other parts of the thin section, away from the large porphyroclasts, record crystal–plastic deformation. Example from the Santa Rosa mylonite zone, Peninsular Ranges batholith, California. (C) Spacing of *S*- and *C*-surfaces and shear bands is determined by the size of the most competent domains, in this case feldspar porphyroclasts. In mylonite (m), foliations are more widely spaced than in phyllonite ultramylonite (u). Only *C*-surfaces are mesoscopically visible in ultramylonite, although *S*-surfaces and pervasive shear bands are evident in thin section (Goodwin and Wenk, 1995).

Material heterogeneity results in differences in strain rate and finite strain magnitude between competence domains that must be accommodated along the domain boundaries. These incompatibilities, if small, can be accommodated by domain-boundary deformation mechanisms. If sufficiently large, however, they produce mechanical instabilities, resulting in the nucleation of micro-shear zones of the type Jordan (1987) documented along domain boundaries in both coaxial and non-coaxial deformation. We propose that movement along these shear zones facilitates the mechanical segregation of the weakest material in the deforming medium by mechanisms that must include some form of domain-boundary sliding (analogous to grain-scale mechanisms proposed by Borradaile, 1981), which will vary with depth (cf. Fig. 4).

The process of formation of compositional bands, and subsequent deformation, both facilitates and is facilitated by strain partitioning. Deformation in shear bands is (at least initially) non-coaxial, even in a coaxially deforming body, due to their orientation with respect to the imposed displacement or stress field. The intervening domains deform with a relatively higher coaxial component of deformation with respect to the micro-shear zones. The domains experiencing dominantly coaxial deformation, however, and those that are deforming noncoaxially are not completely independent of one another. Rather, the magnitude of partitioning will change over time as the domains and the grains within them change orientation (see previous section on competency contrast; Jiang, 1994b). The degree of domain-boundary sliding is fundamentally determined by domain-boundary deformation mechanisms, which are influenced by the magnitude of competency contrast and degree of partitioning between domains as well as environmental factors such as temperature and pressure (Fig. 4).

Competency contrast will thus result in partitioning of flow, regardless of the bulk deformation path. Not only will the strain rate be higher in the incompetent domains, but competent and incompetent domains can follow different deformation paths. This concept has been explored previously, perhaps most elegantly by Lister and Williams (1983) and Jiang (1994b). The former authors noted that competent domains in a rock will experience coaxial deformation while incompetent domains accommodate the non-coaxial component of the flow. The partitioning can occur at any scale of competence domain. This effect is observed, for example, in melts (Handy, 1994; Vigneresse and Tikoff, 1999), shear bands in crystallizing magmas (Nicolas, 1992), and layers of alternating viscosity in experimental studies (Treagus and Sokoutis, 1992).

Lister and Williams (1983) and Jiang (1994b) addressed

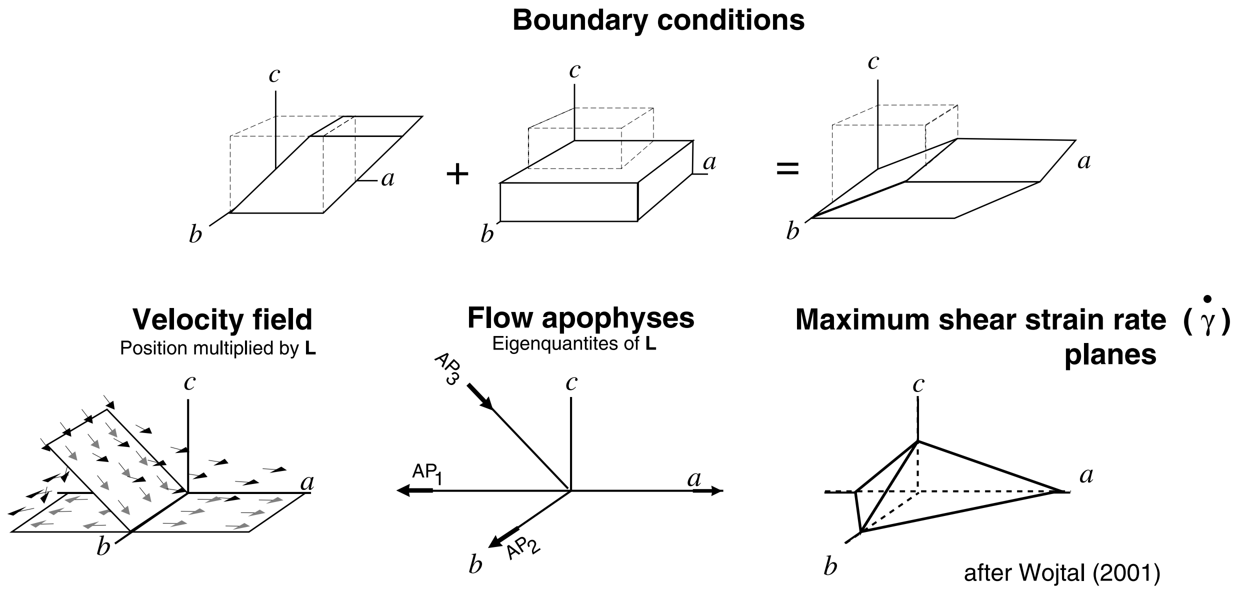

Fig. 8. Diagram demonstrating possible controls on formation of shear surfaces that are not parallel to the *ab* plane. Top: boundary conditions for a three-dimensional general shear. Bottom, from left to right: Velocity field, flow apophyses orientations, and maximum shear strain rate planes for the above deformation. Maximum shear strain rate occurs along four oblique planes that produce a monoclinic symmetry of fault-zone fabric. Zones of localized shear may initiate parallel to planes of maximum shear strain rate (Simpson and De Paor, 1993; Wojtal, 2001).

the implications, but not the processes of development, of mechanical anisotropies such as compositional banding. In contrast, we emphasize the development of compositional banding. In addition, we consider more recent research into general shear in heterogeneous media, which indicates that lineations in ductile shear zones need not track the direction of tectonic transport for three-dimensional deformations (Fossen and Tikoff, 1993; Robin and Cruden, 1994; Jiang and Williams, 1998; Lin et al., 1998).

4.1. Development of shear bands and implications for symmetry

We have proposed that shear bands initiate at competence domain boundaries because of mechanical instabilities that result from strain incompatibilities. We address the orientations of the shear zones formed in this way, and their affect on the symmetry of the resulting fabric, below.

The analysis of kinematic indicators in naturally deformed earth materials is founded on the principle that the symmetry of the fabric is greater than or equal to that of the flow field (Sander, 1930; Turner, 1957; Paterson and Weiss, 1961). Sander (1930) defined three mutually perpendicular kinematic coordinate axes for a rock of monoclinic symmetry, which in many cases records flow dominated by simple shear. The *a* axis is defined as parallel to the transport direction, *b* is parallel to the single axis of rotation, and the *ac*plane is defined by the mirror plane perpendicular to the axis of rotation. Thus, a rock with monoclinic symmetry will exhibit maximum asymmetry on faces parallel to the *ac* plane — the ‘movement plane’ of later workers (e.g. Passchier and Simpson, 1986). Recent studies have considered systems with triclinic symmetry in greater detail (e.g. Robin and Cruden, 1994; Jiang and Williams, 1998; Lin et al., 1998). These models tie the resultant fabric to the kinematic history, either through infinitesimal (e.g. Robin and Cruden, 1994) or finite strain (e.g. Jiang and Williams, 1998; Lin et al., 1998).

In the coordinate system given above, *C*-surfaces are parallel to the *ab* plane, which is an integral part of the flow field (see the following section). Jiang and White (1995) demonstrate that the orientations of *C*-surfaces and shear bands can be controlled by either kinematics or mechanics, and may change with increasing strain, so that it is inappropriate to infer genetics from geometry. Wojtal (2001) suggests that the orientations of shear surfaces in fault zones may be controlled in three-dimensional general shear by kinematic boundary conditions (Fig. 8). In his model, four discrete, non-orthogonal shear surfaces initiate in orientations controlled by the velocity gradient tensor — planes of maximum shear strain rate — and subsequently rotate toward flow apophyses (see the following section). The shear sense on any given surface is not parallel to that of any of the other surfaces, leading to monoclinic symmetry. Other authors have suggested mechanical controls on shear band formation, such as the orientation of a pre-existing foliation relative to the shortening and extension fields of the instantaneous strain ellipsoid (e.g. Williams and Price, 1990).

Regardless of what controls shear band orientation, high competency contrast will result in strain partitioning and the consequent formation of *C*-surfaces and/or shear bands. In contrast, a material lacking or with very low competency contrast will produce a single mesoscopically visible

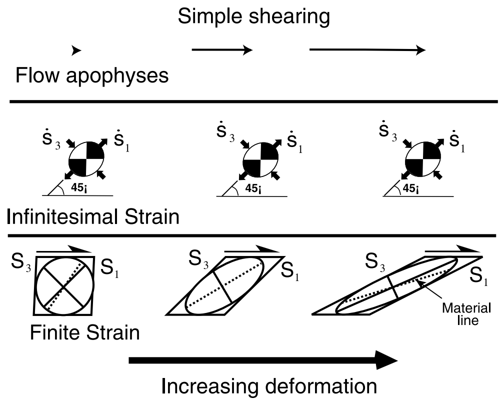

Fig. 9. Flow apophyses, displacement, infinitesimal strain axes, and finite strain axes in two dimensions for a steady-state, simple shear deformation. For simple shearing, both flow apophyses are parallel to the displacement vector, shown with arrows. The magnitudes of both displacement and finite strain change during deformation, whereas both the orientations and lengths of the flow apophyses and infinitesimal strain axes (infinitesimal quantities) are constant during steady-state deformation. Material lines and the finite strain ellipse axes are attracted to the flow apophyses, although individual material lines are attracted more quickly and thus rotate through the long axis of the finite strain ellipse.

foliation. Therefore, a high competency contrast will generally result in a decrease in the symmetry of the rock fabric.

As noted previously, the subsequent segregation of incompetent material into shear bands and *C*-surfaces results in overall strain softening at initial stages in the deformation (e.g. Jordan, 1987). In coaxial deformation, strain softening should theoretically give way to strain hardening at higher strains once a planar compositional banding has developed (e.g. Donath, 1961). In contrast, the compositional banding developed through noncoaxial deformation should facilitate continued deformation.

4.2. Flow apophyses

Once shear surfaces (either shear bands and/or *C*-surfaces) have initiated, the kinematics of flow play a dominant role in the segregation of incompetent material and affect fabric development in different competence domains through deformation partitioning. The consequences of this are most profound where there is a non-coaxial component to the deformation, and we specifically address the effect of strain partitioning on fabric formation in different competence domains. Since partitioning affects the velocity field (Lister and Williams, 1983), the most relevant parameters for quantifying the amount of strain partitioning are those that describe the velocity: the flow apophyses. The term 'flow apophysis' was introduced into the structural geology literature by Ramberg (1975). Essentially, flow apophyses are maximum infinitesimal displacements: there is a direction of maximum infinitesimal convergence and a direction of maximum infinitesimal divergence. There are three flow apophyses in general shear. In simple shear, there are two flow apophyses parallel to the tectonic transport direction in the movement plane (a degenerate case; Bobyarchick, 1986) and one flow apophysis parallel to the vorticity vector and perpendicular to the other flow apophyses. The two parallel flow apophyses for simple shearing are 'neutral', neither moving toward (convergent) nor away from (divergent) the origin.

It is routinely assumed by many workers that finite strain is the kinematic parameter that controls rock fabric. However, material lines and planes rotate toward the flow apophyses, rather than the finite strain axes (Fossen et al., 1994; Passchier, 1997). This effect is observed by noting that an appropriately oriented material line will rotate through an axis of the finite strain ellipse for any non-coaxial deformation (Fig. 9). Material lines rotate through the finite strain ellipse axes because an individual line rotates faster than the aggregate of all lines (i.e. the finite strain ellipse). In fact, for any non-coaxial monoclinic deformation, the finite strain axes themselves rotate from initial parallelism with the infinitesimal strain axes into increasing parallelism with the flow apophyses. The finite strain and material lines are most attracted to the divergent flow apophysis, and thus material moves to that orientation. In transpression (*sensu* Sanderson and Marchini, 1984), for example, one flow apophysis is parallel to the transport direction (neutral), one is vertical (divergent), and one is parallel to the convergence direction (convergent). The flow apophyses are not mutually perpendicular, except for the end-member case of orthogonal convergence. For any transpressional deformation, material lines are generally 'attracted' toward the divergent (vertical) flow apophysis (Fossen et al., 1994). This attraction occurs regardless of the orientation of the infinitesimal strain (e.g. wrench dominated versus pure-shear dominated transpression) or the finite strain. This result is somewhat counterintuitive, as the minimum extensional finite strain axis (S_3) lies in the horizontal plane for some wrench-dominated transpressional deformations. However, this result demonstrates the important point that material lines are attracted to the flow apophyses, rather than infinitesimal strain or finite strain axes.

4.3. Implications for lineations

The partitioning of flow requires that different competence domains in a deforming body be generally described by different flow apophyses. In a hypothetical example, *C*-domains (defining *C*-surfaces) are dominated by non-coaxial shear while the lithons between the *C*-domains are dominated by coaxial flow (Fig. 10). The fabric developed within each domain is dictated by a separate set of flow apophyses, which attract material lines to different orientations at different rates. Two foliations can be stable as a result of the strain partitioning caused by the competency contrast. *S*- and *C*-surfaces in mylonites are familiar examples of foliations that can form simultaneously as strain is partitioned in a single rock (e.g. Berthé et al., 1979).

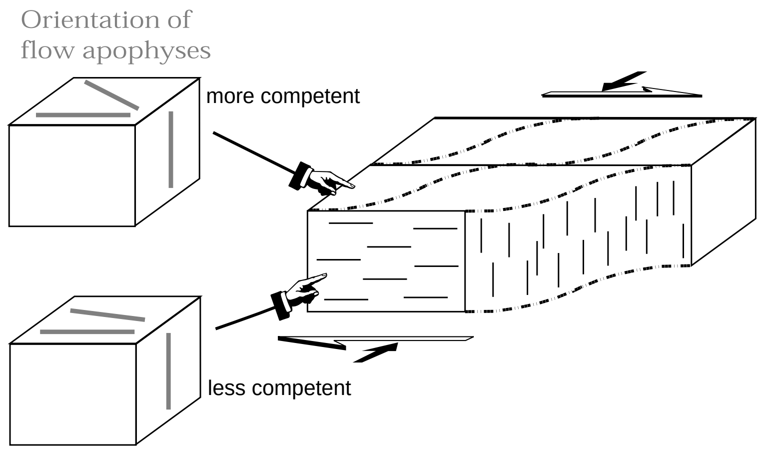

Fig. 10. Orientation of flow apophyses (block diagrams) and lineations within *S*- and *C*-domains within a transpressional shear zone. The less competent *C*-domains are dominated by horizontal lineations, parallel to the horizontal attractor (maximum divergence) flow apophysis. The more competent *S*-domains are characterized by vertical lineations, parallel to the vertical attractor flow apophysis. The deformation partitioning, caused by competency contrast, allows the formation of stable, mutually perpendicular lineations in the different competency domains. Modified from Tikoff and Greene (1997).

Berthé et al. (1979) note that *S*-surfaces initially form close to parallel to the S_1S_2 plane of the finite strain ellipsoid and contain a stretching lineation that is essentially parallel to S_1. The more competent *S*-domains are thus characterized by a stretching lineation that rotates with the foliation. In contrast, the transport direction — implying dominantly non-coaxial deformation — is commonly recorded by ridge-in-groove slickenside striae on *C*-surfaces (e.g. Lin and Williams, 1992b). The transport direction for this type of rock is parallel to the orthogonal projection of the stretching lineation on the *C*-surface, and perpendicular to the intersection between *S*- and *C*-surfaces as long as the movement picture is monoclinic (Lin and Williams, 1992a). The ridge-in-groove slickenside striae developed in the less competent *C*-domains are not only parallel to the transport direction, but record both higher shear strain and higher strain rate than the lineation in *S*-domains. The existence of two lineations in an *S*/*C* mylonite within a simple shear zone makes sense when competency contrast is considered, as *S*- and *C*-domains are characterized by different flow apophyses and attracted to these apophyses at different rates (Figs. 9 and 10). Similar results are seen for bulk coaxial deformation in two dimensions. In Jordan's (1987) coaxial deformation experiments, the less competent halite domains initially deformed non-coaxially within conjugate shear bands. Fabric in these domains presumably records the flow apophyses caused by this local, non-coaxial flow. Note that although these shear bands helped accommodate the overall deformation, the shear-band fabrics will not have a simple relationship to the bulk finite strain.

The consequences of deformation partitioning, which fundamentally results from material heterogeneity, are surprising for three-dimensional general shear. Again, we will consider the example of transpression. Predominantly non-coaxial deformation occurs within the less competent *C*-domains. The boundary conditions of transpression require subhorizontal translation, so that the non-coaxial component of shear localized in the incompetent *C*-domains results in the formation of horizontal ridge-in-groove slickenlines parallel to the transport direction. In contrast, the more competent *S*-domains respond to a different set of flow apophyses. Generally, in transpression, the attractor (maximum divergent) flow apophysis is vertical, therefore vertical lineations will occur in the *S*-domains (e.g. Tikoff and Greene, 1997). Thus, not only do two stable lineations form, but they are perpendicular to one another. High competency contrast can therefore result in the formation not only of multiple foliations, but also of multiple lineations in a single deformational event. The development and orientation of fabric elements in a given competence domain are controlled by the local flow apophyses for steady-state deformation.

5. Conclusions and implications

Polyphase materials are far more common than monophase materials in the Earth's crust; thus, mechanical heterogeneity represents the general case in naturally deformed rocks. A fundamental consequence of this heterogeneity is that deformation will produce strain and strain-rate variations between competence domains. The degree of strain and strain-rate incompatibilities produced along domain boundaries will be dictated by the magnitude of competency contrast. Where competency contrast is high, small domain-boundary adjustments are insufficient to accommodate incompatibilities, and strain in the competent domains will be localized in micro-shear zones. The number and orientations of these shear zones — conjugate shear bands versus a single orientation of shear bands and/or *C*-surfaces — will reflect the flow field and the mechanics of the system regardless of the deformation mechanisms that accommodated flow. The initiation of these structures is both the result of, and facilitates, deformation partitioning, with noncoaxial shear preferentially accomplished by shear bands and *C*-surfaces and the intervening domains preferentially accommodating the coaxial component of flow.

From a kinematic viewpoint, the degree of strain partitioning is directly proportional to the magnitude of competency contrast between mechanically distinct domains. A result of this partitioning in three-dimensional general shear such as transpression is that lineations can form in very different orientations in adjacent domains if competency contrast is high. Thus, the transport direction is most likely to be recorded by a lineation developed in the least competent domains in the system. Large competency contrasts are more likely to decrease the symmetry of the flow system, and therefore the fabric, for a given set of boundary conditions. The more competent domains will record a three-dimensional shape (constriction, flattening, plane strain) and internal fabric that constrains the geometry of the flow in these domains (Hudleston, 1999). The symmetry of the system of domains, and internal fabrics of domains, can be used in conjunction with the transport lineation to determine the sense of shear. In the most extreme case, a lineation in an incompetent domain can be perpendicular to one in a competent domain.

The above example suggests that, because polyphase materials are more likely to have high competency contrast, they have a greater potential for providing a more complete record of the flow field than monophase materials. They may also provide a superior record of rheology. Previous workers have used the form and orientation of geologic structures to infer the possible rheologies of rocks during deformation (e.g. Cobbold, 1983; Treagus and Sokoutis, 1992; Hudleston and Lan, 1995; Treagus and Lan, 2000). If we consider the same approach here, it is evident that there are three elements that might collectively provide a record of rheology: (1) the three-dimensional patterns of foliations, lineations, and CPO within competence domains; (2) the three-dimensional morphology of competence domains; and (3) microstructures that record strain rates within and between competence domains. The domainal character of natural materials, which allows structures in relatively deep crustal shear zones to develop in a manner similar to structures in true granular materials, such as faulted unlithified sediments, is key to understanding the development of compositional foliation banding and the rheology of natural systems.

A strength of our approach is that it is largely scale independent, as neither competency contrast nor kinematic history is tied to any particular scale of deformation. This suggests that the resultant patterns of deformation can occur at a variety of scales.

Acknowledgements

This paper grew out of an informal discussion with Steven Ralser, on a Saturday afternoon in Socorro, in which we questioned what we really knew about lineation development. Support for this research was provided by NSF grant EAR-9706482 to LBG and a Packard Foundation grant to BT. Cheryl Waters suffered through very rough drafts of this manuscript, and suggested significant improvements. Michelle Markley, Steven Ralser, and Shannon Baer provided helpful comments on later drafts, for which we are grateful. Official reviews provided by Joseph White, Richard Law, and Ben van der Pluijm were exceptionally thoughtful and thorough, and improved the manuscript dramatically. Scott Johnson and Mike Williams provided the impetus for presenting these ideas in a public forum, which led to the development of this paper, and provided a final, helpful review. Peter Hudleston and Dyanna Czeck are thanked for a helpful conversation about competency contrast. Win Means provided both general inspiration and specific criticisms. We would like to dedicate this paper to Ron Vernon (whether he likes it or not), whose example of integrating different sub-disciplines, open mindedness, and enthusiasm is an inspiration to us all.

References

Agar, S.M., Prior, D.J., Behrmann, J.H., 1989. Back-scattered electron imagery of the tectonic fabrics of some fine-grained sediments: implications for fabric nomenclature and deformation processes. Geology 17, 901–904.

Behringer's Nonlinear Flow Group, 2001. http://www.phy.duke.edu/research/ltb/ltbgroup.html.

Bell, T.H., Rubenach, M.J., Fleming, P.D., 1986. Porphyroblast nucleation, growth and dissolution in regional metamorphic rocks as a function of deformation partitioning during foliation development. Journal of Metamorphic Geology 4, 37–47.

Berthé, D., Choukroune, P., Jegouzo, P., 1979. Orthogneiss, mylonite and non-coaxial deformation of granites: the example of the South American shear zone. Journal of Structural Geology 1, 31–42.

Bobyarchick, A.R., 1986. The eigenvalues of steady flow in Mohr space. Tectonophysics 122, 35–51.

Borradaile, G.J., 1981. Particulate flow of rock and the formation of cleavage. Tectonophysics 72, 305–321.

Brandon, M.T., Cowan, D.S., Feehan, J.G., 1994. Fault-zone structures and solution-mass-transfer cleavage in Late Cretaceous nappes, San Juan Islands, Washington. In: Swanson, D.A., Haugerud, R.A. (Eds.). Geologic Field Trips in the Pacific Northwest. 1994 Geological Society of America Annual Meeting, Seattle, Washington, pp. 2L1–19.

Chester, F.M., Friedman, M., Logan, J.M., 1985. Foliated cataclasites. Tectonophysics 111, 139–146.

Cladouhos, T., 1999. Shape preferred orientations of survivor grains in fault gouge. Journal of Structural Geology 21, 419–436.

Cobbold, P.R., 1977. Description and origin of banded deformation structures. I. Regional strain, local perturbations, and deformation bands. Canadian Journal of Earth Science 14, 1721–1731.

Cobbold, P.R., 1983. Kinematic and mechanical discontinuity at a coherent interface. Journal of Structural Geology 5, 341–349.

Connell, S.D., Koning, D.J., Cather, S.M., 1999. Revisions to the statrigraphic nomenclature of the Santa Fe Group, northwestern Albuquerque Basin, New Mexico. In: Pazzaglia, F.J., Lucas, S.G.

(Eds.). Albuquerque Geology. New Mexico Geological Society Guidebook 50, pp. 337–353.

Cosgrove, J.W., 1976. The formation of crenulation cleavage. Journal of the Geological Society, London 132, 155–178.

Dennis, J.G. (Ed.), 1967. International Tectonic Dictionary: English Terminology. International Geological Congress, Memoir 7.

DeVore, G.W., 1969. Preferred mineral distributions of polymineralic rocks related to non-hydrostatic stresses as expressions of mechanical equilibria. Journal of Geology 77, 26–38.

Donath, F.A., 1961. Experimental study of shear failure in anisotropic rocks. Geological Society of America Bulletin 72, 985–990.

Etheridge, M.A., Wilkie, J.C., 1979. Grainsize reduction, grain boundary sliding and the flow strength of mylonites. Tectonophysics 58, 159–178.

Evans, J.P., 1988. Deformation mechanisms in granitic rocks at shallow crustal levels. Journal of Structural Geology 10, 437–443.

Flinn, D., 1969. Grain contacts in crystalline rocks. Lithos 3, 361–370.

Fossen, H., Tikoff, B., 1993. The deformation matrix for simultaneous pure shear, simple shear, and volume change, and its application to transpression/transtension tectonics. Journal of Structural Geology 15, 413–425.

Fossen, H., Tikoff, B., Teyssier, C., 1994. Strain modeling of transpressional and transtensional deformation. Norsk geologisk Tidsskrift 74, 134–145.

Gapais, D., White, S.H., 1982. Ductile shear bands in a naturally deformed quartzite. Textures and Microstructures 5, 1–17.

Goodwin, L.B., 1999. Controls on pseudotachylyte formation during tectonic exhumation in the South Mountain metamorphic core complex, Arizona. In: Uwe, R., Brandon, M.T., Lister, G.S., Willett, S.D. (Eds.). Exhumation Processes, Normal Faulting, Ductile Flow, and Erosion. Geological Society Special Publication 154, pp. 325–342.

Goodwin, L.B., O'Neill, P.P., 1991. The structural evolution of the northern segment of the Dunnage zone/Gander zone boundary, Newfoundland. Lithoprobe Report 13, 64–74.

Goodwin, L.B., Wenk, H.R., 1995. Development of phyllonite from granodiorite; mechanisms of grain-size reduction in the Santa Rosa mylonite zone, California. Journal of Structural Geology 17, 689–707.

Gray, D.R., Durney, D.W., 1979. Crenulation cleavage differentiation: implication of solution — deposition processes. Journal of Structural Geology 1, 73–80.

Handy, M.R., 1990. The solid-state flow of polymineralic rocks. Journal of Geophysical Research 95, 8647–8661.

Handy, M.R., 1994. Flow laws for rocks containing two nonlinear viscous phases: a phenomenological approach. Journal of Structural Geology 16, 287–301.

Hanmer, S., Williams, M., Kopf, C., 1995. Modest movements, spectacular fabrics in an intracontinental deep-crustal strike-slip fault: striding-Athabasca mylonite zone, NW Canadian Shield. Journal of Structural Geology 17, 493–507.

Hawley, J.W., 1996. Hydrogeologic framework of potential recharge areas in the Albuquerque Basin, central New Mexico. New Mexico Bureau of Mines and Mineral Resources Open-File Report 402 D, Chapter 1.

Hawley, J.W., Haase, C.S., Lozinsky, R.P., 1995. An underground view of the Albuquerque Basin. In: The Water Future of Albuquerque and the Middle Rio Grande Basin (Proceedings of the 39th Annual New Mexico Water Conference). New Mexico Water Resources Research Institute Report 290, pp. 37–55.

Heynekamp, M.R., Goodwin, L.B., Mozley, P.S., Haneberg, W.C., 1999. Controls on fault-zone architecture in poorly lithified sediments, Rio Grande Rift, New Mexico: implications for fault-zone permeability and fluid flow. In: Haneberg, W.C., Mozley, P.S., Moore, J.C., Goodwin, L.B. (Eds.). Faults and Subsurface Fluid Flow in the Shallow Crust. AGU Monograph 113, pp. 27–49.

Hudleston, P.J., 1999. Strain compatibility and shear zones; is there a problem? Journal of Structural Geology 21, 923–932.

Hudleston, P.J., Lan, L., 1995. Rheological information from geological structures. Pageoph 145, 605–620.

Jiang, D., 1994a. Vorticity determination, distribution, partitioning and the heterogeneity and non-steadiness of natural deformations. Journal of Structural Geology 16, 121–130.

Jiang, D., 1994b. Flow variation in layered rocks subjected to bulk flow of various kinematic vorticities: theory and geological implications. Journal of Structural Geology 16, 1159–1172.

Jiang, D., White, J.C., 1995. Kinematics of rock flow and the interpretation of geological structures, with particular reference to shear zones. Journal of Structural Geology 17, 1249–1265.

Jiang, D., Williams, P.F., 1998. High-strain zones: a unified model. Journal of Structural Geology 20, 1105–1120.

Jordan, P., 1987. The deformational behaviour of bimineralic limestone–halite aggregates. Tectonophysics 135, 185–197.

Kanaori, Y., Kawakami, S., Yairi, K., 1991. Microstructure of deformed biotite defining foliation in cataclasite zones in granite, central Japan. Journal of Structural Geology 13, 777–786.

Knipe, R.J., 1989. Deformation mechanisms — recognition from natural tectonites. Journal of Structural Geology 11, 127–146.

Knipe, R.J., 1986. Faulting mechanisms in slope sediments: examples from Deep Sea Drilling Project Cores. In: Moore, J.C. (Ed.). Structural Fabric in Deep Sea Drilling Project Cores from Forearcs. Geological Society of America Memoir 166, pp. 45–54.

Knipe, R.J., Wintsch, R.P., 1985. Heterogeneous deformation, foliation development and metamorphic processes in a polyphase mylonite. In: Thompson, A., Rubie, D.C. (Eds.). Kinetics, Textures and Deformation. Springer, New York. Advances in Physical Geochemistry, 4, pp. 180–210.

Labaume, P., Maltman, A.J., Bolton, A., Tessier, D., Ogawa, Y., Takizawa, S., 1997. Scaley fabrics in sheared clays from the decollement zone of the Barbados accretionary prism. In: Shipley, T.H., Ogawa, Y., Blum, P., Bahr, J.M. (Eds.). Proceedings of the Ocean Drilling Program. Scientific Results 156, pp. 59–77.

Law, R.D., Casey, M., Knipe, R.J., 1986. Kinematic and tectonic significance of microstructures and crystallographic fabrics within quartz mylonites from the Assynt and Eriboll regions of the Moine thrust zone, NW Scotland. Transactions of the Royal Society of Edinburgh: Earth Sciences 77, 99–125.

Law, R.D., Knipe, R.J., Dayan, H., 1984. Strain path partitioning within thrust sheets: microstructural and petrograbric evidence from the Moine Thrust zone at Loch Eriboll, northwest Scotland. Journal of Structural Geology 6, 477–497.

Lin, S., Williams, P.F., 1992a. The geometrical relationship between the stretching lineation and the movement direction of shear zones. Journal of Structural Geology 14, 491–497.

Lin, S., Williams, P.F., 1992b. The origin of ridge-in-groove slickenside striae and associated steps in an *S–C* mylonite. Journal of Structural Geology 14, 315–321.

Lin, S., Jiang, D., Williams, P.F., 1998. Transpression (or transtension) zones of triclinic symmetry: natural examples and theoretical modeling. In: Holdsworth, R.E., Strachan, R.A., Dewey, J.F. (Eds.). Continental Transpressional and Transtensional Tectonics. Geological Society Special Publication 135, pp. 41–57.

Lister, G.S., Williams, P.F., 1983. The partitioning of deformation in flowing rock masses. Tectonophysics 92, 1–33.

Logan, J.M., Dengo, C.A., Higgs, N.G., Wang, Z.Z., 1992. Fabrics of experimental fault zones: their development and relationship to mechanical behavior. In: Evans, B., Wong, T.-F. (Eds.). Fault Mechanics and Transport Properties of Rocks. Academic Press, London, pp. 33–68 International Geophysics Series 51.

Lohr, M., Yamagata, T., Moore, J.C., 1999. Structural fabrics and hydrocarbon content of the San Gregorio Fault Zone, Moss Beach California. In: Garrison, R.E., Aiello, I., Moore, J.C. (Eds.). Late Cenozoic Fluid Seeps and Tectonics Along the San Gregorio Fault Zone in the Monterey Bay Region, California. American Association of Petroleum Geologists, Pacific Section, Bakersfield, CA, pp. 21–34 Guidebook 76.

Maltman, A., Labaume, P., Housen, B., 1997. Structural geology of the decollement at the toe of the Barbados accretionary prism. In: Shipley, T.H., Ogawa, Y., Blum, P., Bahr, J.M. (Eds.). Proceedings of the Ocean Drilling Program. Scientific Results 156, pp. 279–292.

Means, W.D., 1977. Experimental contributions to the study of foliations in rocks; a review of research since 1960. Tectonophysics 39, 329–354.

Means, W.D., 1995. Shear zones and rock history. Tectonophysics 247, 157–160.

Means, W.D., Williams, P.F., 1972. Crenulation cleavage and faulting in an artificial salt–mica schist. Journal of Geology 80, 569–571.

Means, W.D., Williams, P.F., 1974. Compositional differentiation in an experimentally deformed salt–mica specimen. Geology 2, 15–16.

Moore, J.C., Roeske, S.M., Lundberg, N., Schoonmaker, J., Cowan, D.S., Gonzales, E., Lucas, S.E., 1986. Scaly fabrics from Deep Sea Drilling Project cores from forearcs. In: Moore, J.C. (Ed.). Structural Fabric in Deep Sea Drilling Project Cores from Forearcs. Geological Society of America Memoir 166, pp. 55–73.

Mozley, P.S., Goodwin, L.B., 1995. Patterns of cementation along a Cenozoic normal fault: a record of paleoflow orientations. Geology 23, 539–542.

Nicolas, A., 1992. Kinematics in magmatic rocks with special reference to gabbros. Journal of Petrology 33, 891–915.

O'Hara, K., 1988. Fluid flow and volume loss during mylonitization: an origin for phyllonite in an overthrust setting, North Carolina, USA. Tectonophysics 156, 21–36.

Passchier, C.W., 1997. The fabric attractor. Journal of Structural Geology 19, 113–127.

Passchier, C.W., Simpson, C., 1986. Porphyroclast systems as kinematic indicators. Journal of Structural Geology 8, 831–844.

Passchier, C.W., Trouw, R.A.J., 1996. Microtectonics. Springer, Berlin 289pp.

Paterson, M.S., Weiss, L.E., 1961. Symmetry concepts in the structural analysis of deformed rocks. Geological Society of America Bulletin 72, 841–882.

Platt, J.P., 1979. Extensional crenulation cleavage. Journal of Structural Geology 1, 95.

Platt, J.P., Vissers, R.L.M., 1980. Extensional structures in anisotropic rocks. Journal of Structural Geology 2, 397–410.

Ponce de Leon, M.J., Choukroune, P., 1980. Shear zones in the Iberian arc. Journal of Structural Geology 2, 63–68.

Ralser, S., Hobbs, B.E., Ord, A., 1991. Experimental deformation of a quartz mylonite. Journal of Structural Geology 12, 1033–1045.

Ramberg, H., 1975. Particle paths, displacement and progressive strain applicable to rocks. Tectonophysics 28, 1–37.

Rawling, G.C., Goodwin, L.B., Wilson, J.L., 2001. Internal architecture, permeability structure, and hydrologic significance of contrasting fault-zone types. Geology 29, 43–46.

Robin, P.-Y.F., Cruden, A.R., 1994. Strain and vorticity patterns in ideally ductile transpression zones. Journal of Structural Geology 16, 447–466.

Rutter, E.H., Maddock, R.H., Hall, S.H., White, S.H., 1986. Comparitive microstructures of natural and experimentally produced clay-bearing fault gouges. Pageoph 124, 3–30.

Sander, B., 1930. Gefugekunde der Gesteine. Springer-Verlag OHG, Vienna.

Sanderson, D., Marchini, R.D., 1984. Transpression. Journal of Structural Geology 6, 449–458.

Shea, W.T., Kronenberg, A.K., 1993. Strength and anisotropy of foliated rocks with varied mica contents. In: Kirby, S.H., Sylvester, A.G., Tullis, J., Wenk, H.-R., Treagus, S.H. (Eds.). Microstructures and Rheology of Rocks and Rock-Forming Minerals; A Collection of Papers in Honor of John Christie's 60th Birthday. Journal of Structural Geology 15, pp. 1097–1121.

Shelley, D., 1995. Asymmetric shape preferred orientations as shear-sense indicators. Journal of Structural Geology 17, 509–517.

Shinbrot, T., Muzzio, F.J., 2000. Nonequilibrium patterns in granular mixing and segregation. Physics Today 53, 25–30.

Simpson, C., De Paor, D.G., 1993. Strain and kinematic analysis in general shear zones. Journal of Structural Geology 15, 1–20.

Takeshita, T., Wenk, H.-R., 1988. Plastic anisotropy and geometrical hardening in quartzites. Tectonophysics 149, 345–361.

Tedford, R.H., Barghoorn, S., 1999. Santa Fe Group (Neogene), Ceja del Rio Puerco, Northwestern Albuquerque Basin, Sandoval County, New Mexico. In: Pazzaglia, F.J., Lucas, S.G. (Eds.). Albuquerque Geology. New Mexico Geological Society Guidebook 50, pp. 327–335.

Tikoff, B., Teyssier, C., 1994. Strain modeling of displacement-field partitioning in transpressional orogens. Journal of Structural Geology 16, 1575–1588.

Tikoff, B., Greene, D., 1997. Stretching lineations in transpressional shear zones. Journal of Structural Geology 19, 29–40.

Tikoff, B., St. Blanquat, M., 1997. Transpressional deformation and changing kinematics in the Late Cretaceous Sierra Nevada magmatic arc, California. Tectonics 16, 442–459.

Treagus, S.H., Sokoutis, D., 1992. Laboratory modeling of strain variations across rheological boundaries. Journal of Structural Geology 14, 405–424.

Treagus, S.H., Lan, L., 2000. Pure shear deformation of square inclusions, and applications to geological strain analysis. Journal of Structural Geology 21, 105–122.

Tullis, J., 1990. Experimental studies of deformation mechanisms and microstructure in quartzo-feldspathic rocks. In: Barber, D.J., Meredith, P.G. (Eds.). Deformation Processes in Minerals, Ceramics and Rocks. Unwin Hyman, London, UK, pp. 190–227.

Tullis, J., Yund, R.A., 1985. Dynamic recrystallization of feldspar: a mechanism for ductile shear zone formation. Geology 13, 238–241.

Turner, F.J., 1957. Lineation, symmetry, and internal movement in monoclinic tectonite fabrics. Geological Society of America Bulletin 68, 1–17.

Turner, F.J., Weiss, L.E., 1963. Structural Analysis of Metamorphic Tectonites. McGraw-Hill, New York, 545 pp.

Van Hise, C.R., 1896. Primary and secondary structures and the forces that produced them. Science 3, 294–295.

Vernon, R.J., 1974. Controls of mylonitic compositional layering during non-cataclastic ductile deformation. Geological Magazine 111, 121–123.

Vigneresse, J.-L., Tikoff, B., 1999. Strain partitioning and percolation effects on the rheology of felsic partial melts and crystallizing magmas. Tectonophysics 312, 117–132.

White, J.C., 1982. Quartz deformation and the recognition of recrystallization regimes in the Flinton Group conglomerates, Ontario. Canadian Journal of Earth Sciences 19, 81–93.

White, J.C., Mawer, C.K., 1992. Deep-crustal deformation textures along megathrusts from Newfoundland and Ontario; implications for microstructural preservation, strain rates, and strength of the lithosphere. Canadian Journal of Earth Sciences 29, 328–337.

White, S.H., Knipe, R.J., 1978. Microstructure and cleavage development in selected slates. Contributions to Mineralogy and Petrology 66, 165–174.

White, S.H., Burrows, S.E., Carreras, J., Shaw, N.D., Humphreys, F.J., 1980. On mylonites in ductile shear zones. Journal of Structural Geology 2, 175–187.

Wibberly, C., 1999. Are feldspar-to-mica reactions necessarily reaction-softening processes in fault zones? Journal of Structural Geology 21, 1219–1227.

Williams, P.F., 1977. Foliation; a review and discussion. Tectonophysics 39, 305–328.

Williams, P.F., 1990. Differentiated layering in metamorphic rocks. Earth-Science Reviews 29, 267–281.

Williams, P.F., Price, G.P., 1990. Origin of kinkbands and shear-band cleavage in shear zones: an experimental study. Journal of Structural Geology 12, 145–164.

Willis, B., 1893. The mechanics of Appalachian structure. United States Geological Survey Annual Report 13, 211–281.

Wintsch, R.P., 1985. The possible effects of deformation on chemical processes in metamorphic fault zones. In: Thompson, A., Rubie, D.C.

(Eds.). Kinetics, Textures and Deformation. Springer, New York, pp. 251–268 Advances in Physical Geochemistry, 4.

Wintsch, R.P., Christoffersen, R., Kronenberg, A.K., 1995. Fluid-rock reaction weakening of fault zones. Journal of Geophysical Research 100, 13,021–13,032.

Wojtal, S.F., 2001. The nature and origin of asymmetric arrays of shear surfaces in fault zones. In: Holdsworth, R.E., Strachan, R.A., Magloughlin, J.F., Knipe, R.J. (Eds.). The Nature and Tectonic Significance of Fault Zone Weakening. Journal of the Geological Society, London in press.

Zhang, S.Q., Karato, S., 1995. Lattice preferred orientation of olivine aggregates deformed in simple shear. Nature 375, 774–777.